Meteorol. Atmos. Phys. 74, 159–187 (2000)

Meteorology and Atmospheric Physics

Department of Marine, Earth and Atmospheric Sciences, North Carolina State University, Raleigh, NC

Mesoscale simulations of dynamical factors discriminating between a tornado outbreak and non-event over the southeast US Part II: 48-6 hour precursors

J. M. Egentowich, M. L. Kaplan, Y.-L. Lin, and **A. J. Riordan**

With 26 Figures

Received December 23, 1999
Revised January 16, 2000

Summary

Using observational analysis and mesoscale numerical simulations we investigate the subtropical jet (STJ) and its effects on the lower environment (associated mass and momentum adjustments, development of a low-level jet (LLJ), and low-level PV) 48 to 6 hours before the Raleight tornado outbreak (1988). We also compare the environment to a synoptically similar event in which severe weather forecasted but did not develop over central North Carolina. In the severe weather case a self-maintaining. low-level circulation originated over Mexico, propagated across the Gulf Coast and moved over the Piedmont at the time of the tornado. It is characterized by a surface trough, low-level PV maximum, mid-level jet, a warm Mexican airmass and STJ exit region that was co-located and moved across the Gulf Coast States as a coupled system. Initially, a STJ exit region (with thermally indirect ageostrophic circulation) approached the Gulf Coast creating upper-level divergence and ascent, which helped to maintain a low-level trough. A warm Mexican airmass was located over the Gulf Coast (southeast of the surface trough) creating a northwestward-directed PGF, which created a mid-level jet. The right entrance region of the mid-level jet and its associated thermally direct circulation (ascent) was over the low-level trough. These features created an environment favorable to deep convection and the release of latent heat that generated low-level PV. In the non-event case, these features (low-level warm Mexican airmass, mid-level jet, deep convection, low-level PV and low-level trough) were absent over the Gulf Coast States.

1. Introduction

The Raleigh, North Carolina tornado of 28 November 1988 was an extraordinary event, which has stimulated a great deal of interest from the weather forecasting and research communities. The National Weather Service didn't issuing *any* severe weather watch or warning prior to observations of severe weather, in part, because the severe weather predictive indices based upon typical jet exit region dynamics were unremarkable (Gonski, 1989). This second part of a three part series examines 48 to 6 hours before a tornado event and compares it to a synoptically similar non-event.

Kaplan et al. (1998) proposed a new severe weather paradigm with three primary components which we apply in these cases. First, the juxtapositioning of the PJ entrance region and the subtropical jet (STJ) exit region and their transverse secondary circulations create deep QG vertical motions. Second, the adjustment of the mass field to the subgeostrophic wind field occurs in proximity to the continental air and polar air interface, i.e., low-level fronts accompany the return branch of the STJ streak and

return branch of the PJ streak resulting in midtropospheric mesoscale jet streak. Third, air parcels are subjected to intensifying stretching and tilting as they are caught up in the thermally direct unbalanced circulation in the right front quadrant of the adjusting jetlet.

The classic "loaded gun" type 1 tornado sounding, (Fawbush and Miller, 1954) has a moist unstable layer capped by an elevated mixed layer (EML). The EML creates a large area of instability. Lanici and Warner (1991) performed an in-depth lid study that examines the EML source region of Mexico. They examined the climatology, characteristics, life cycle, and relationship to severe storms. They assume the lid is a feature that facilitates intense convection by greatly increasing the convective instability. *We hypothesize that the warm air off the Mexican plateau (EML) not only creates convective instability but also forces a geostrophic adjustment process that creates a mid-level jet, which maintains a propagating surface trough and facilitates strong convection.*

A hydrostatic environment rich in potential vorticity (PV) is likely to be an environment favoring cyclonic vorticity intensification. Potential vorticity, therefore, is an excellent tracer for the potential rotational energy if it can be combined with an environment favorable for convection. Messoscale PV generation is examined using the Lagrangian PV equation (Gidel and Shapiro, 1979) and may be estimated by:

$$\frac{d}{dt}\left[-(\zeta_\theta + f)\frac{\partial \theta}{\partial p}\right] = \underbrace{-(\zeta_\theta + f)\frac{\partial}{\partial p}\left(\frac{d\theta}{dt}\right)}_{1} \underbrace{-\left(\frac{\partial \theta}{\partial p}\right)\hat{k}\cdot\nabla_\theta \times \vec{F}}_{2} + \underbrace{\left(\frac{\partial \theta}{\partial p}\right)\hat{k}\cdot\nabla_\theta\left(\frac{d\theta}{dt}\right)\times\frac{\partial \vec{V}}{\partial \theta}}_{3}. \quad (1)$$

Term 1 defines the mechanism of PV production or destruction due to vertical gradients of diabatic heating with isentropic absolute vorticity. Term 2 represents the change in PV resulting from frictional stresses. Term 3 represents the change in PV resulting from the tilting of the horizontal component of vorticity into the vertical through horizontally varying diabatic heating. Gyakum et al. (1995) related the diabatic PV production to rapid surface cyclogenesis, concluding that surface frontogenesis produced a vertical wind shear enhancing the diabatic generation of PV through tilting. Zehnder and Keyser (1991) investigated rapid cyclogenesis in the absence of diabatic effects. They found the interaction between upper- and lower-level disturbances characterized by nonuniform PV results in a significant increase in relative vorticity at the surface.

Egentowich et al. (1999) (in this issue Part 1) compare the event (RDU tornado, 28 November 1988) to a non-event (25 January 1990), discusses the early synoptic situation (84-48 hours before the event and non-event), jet development, low-level PV development and warm air transport. In the event case, upper-level jetogenesis creates a STJ streak over TX and MX. The transverse ageostrophic circulation associated with the STJ forces air down the eastern side of the Sierra Madre Mountains creating adiabatic warming due to compressional heating, which creates a low-level trough and a low-level jet (LLJ) over the western Gulf of Mexico. The LLJ transports very warm low-level air from the Mexican plateau to the Gulf Coast. The non-event case has a different synoptic pattern; the upper-level flow is very zonal over the US with a ridge over MX. A PJ develops over northern TX, OK and MO and the ridge prevents the STJ from developing or moving over the Gulf of Mexico. During the early period, no transport mechanism (LLJ) develops to move the hot air off the Mexican plateau.

For the event case, the STJ exit region and its associated thermally indirect circulation transports the PV down to the midlevels over the Mexican plateau. At the same time, a mountain-plains solenoid (MPS) develops due to strong heating over the Mexican plateau creating ascent and an area of strong vertical convergence, which increases the thermal gradient (static stability) and generates PV. This midlevel PV maximum moves eastward and a hydrostatic mountain wave transports the PV downward near the Mexican coast. The low-level PV then moves northeastward along the Gulf Coast. In the non-event, the STJ is absent, thus PV is not transported downward to the midlevels. The easterly low-level wind field over the western Gulf of Mexico advects clouds inhibiting the development of a

MPS and mountain waves east of the Sierra Madre mountains.

This second paper compares the cases during the period 48 to 6 hours before the event/non-event. In the event case, a surface trough, low-level PV maximum, mid-level jet, a warm Mexican airmass and STJ exit region are co-located and move across the Gulf Coast States as a coupled circulation system. Initially, a STJ exit region approaches the Gulf Coast creating upper-level divergence and ascent in the left exit region, which helps to maintain a low-level trough. The warm Mexican airmass is located over the Gulf Coast creating a mid-level, northwestward directed PGF and a mid-level jet. The mid-level jet entrance region has an associated thermally direct ageostrophic circulation, which further enhances ascent over the low-level trough. These features create an environment favorable for deep convection releasing latent heat, generating low-level PV and produce a self-sustaining circulation that moves across the Gulf Coast States and over central North Carolina at the time of the tornado outbreak. In the non-event case, these features (low-level warm Mexican airmass, mid-level jet, deep convection, low-level PV and low-level trough) are absent along the Gulf Coast States.

In this paper, we explore the relationship between the STJ and its effects on the lower environment (associated mass and momentum adjustments), development of a LLJ, and low-level PV) 48-6 hours before the development of severe weather. We also compare the environment to a synoptically similar event in which severe weather was forecast but did not developed near RDU. In Section 2 we briefly describe the mesoscale model used for the simulations. Section 3 deals with the development of the jet streaks in both the event and non-event. Section 4 focuses on the development and movement of the surface trough (convergence zone) across the Gulf Coast. In Section 5 we investigate the origins of low-level PV. In Section 6 we summarize and present our conclusions.

2. Model summary

Due to the lack of high-resolution observational data, numerical simulations are employed to understand the environments prior to the event and non-event. The MASS model (Kaplan et al., 1982) version 5.8 (MESO, 1995) produces the simulations for this study. The numerical experiments, grid resolution and coverage are summarized in Part 1 (Egentowich et al., 1999). Three-dimensional parcel trajectories used throughout this paper are derived from the Mesoscale Atmospheric Simulation System Trajectory (MASSTRAJ) software package (Rozumalski, 1997).

3. Jet development

3.1 Upper-level jet streams

As in Part 1, one of the most significant differences between the two cases is the presence of the STJ in the event case and its absence in the non-event case. In the event case (0000 UTC 26 November 1988 to 0000 UTC 28 November 1988), the jet streams remain in roughly the same locations over North America. The STJ stream extends from the southeastern Pacific across Central Mexico and the southeast US. The PJ stream extends from northwestern Canada southeast over TX and northward over the Mid-Atlantic States. Individual streaks move through the jet streams, which changes the convergence/divergence areas, the ageostrophic circulations and vertical motions. The non-event case from 1200 UTC 23 January 1990 until about 1200 UTC 25 January 1990 has an upper-level ridge over Mexico, which prevents the development of the STJ. The PJ develops over northern TX and extends over the northeast US. As the upper-level trough develops over the central US, the PJ dips into central TX and extends over the northeast US. These features are examined and related to the low-level environment.

3.1.1 Event case and non-event case observations

Observed data highlight the differences between the event and non-event case and the relationship between the upper-level jets and areas of convection. Figure 1 is the 200 hPa NWS analyses and cross sections valid 0000 UTC 27 November 1988 and 1200 UTC 24 January 1990. Figure 2 is the radar summary valid 0035 UTC 27 November 1988 and 1235 UTC 24 January 1990. For these time periods, eastern TX, LA and MS is the area

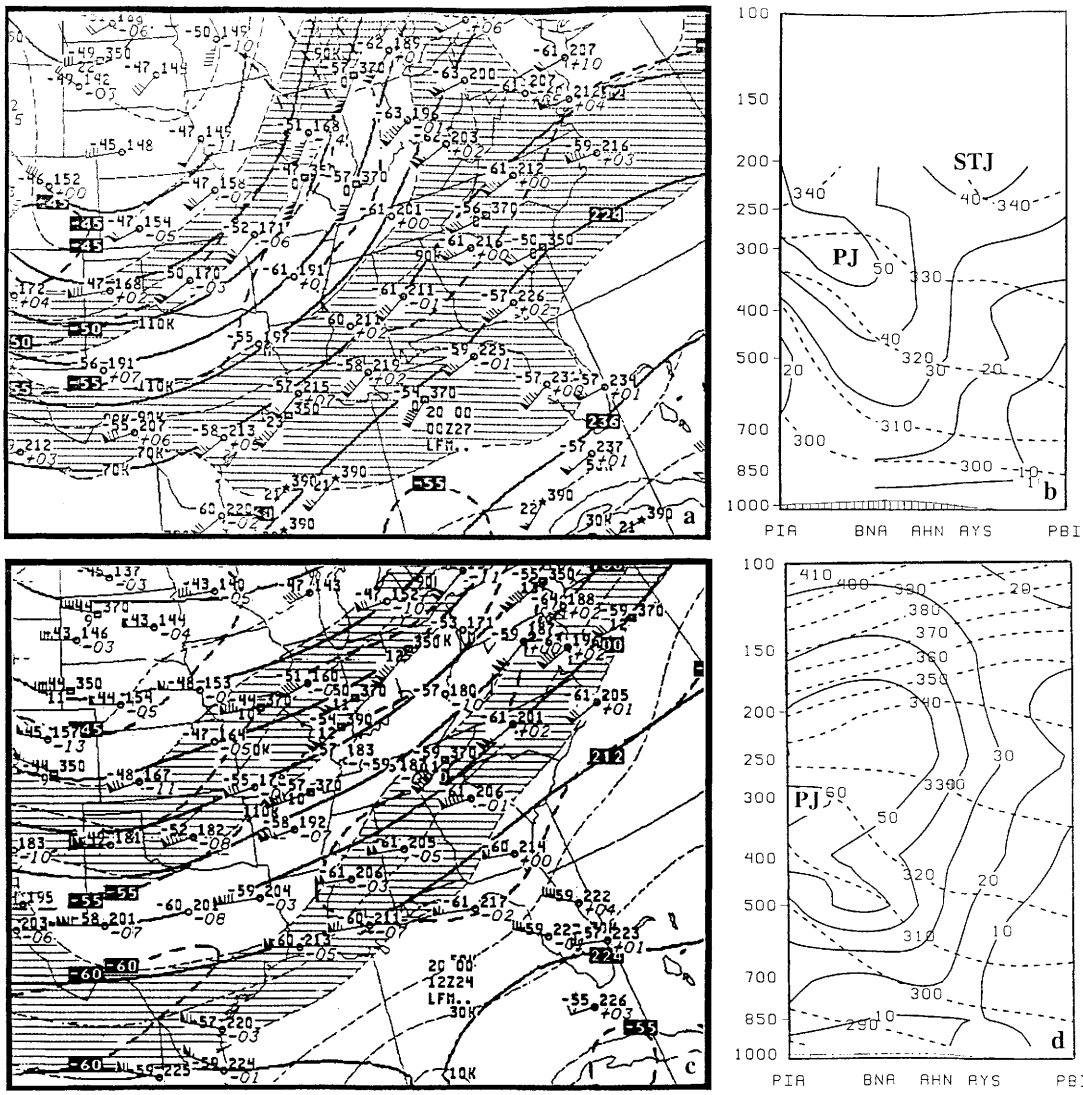

Fig. 1. NWS 200 hPa analysis including isotachs (knots) and vectors, temperature (C) and height (dm) and observation derived cross section from Peoria, IL (PIA) to West Palm Beach, FL (PBI), isotachs (solid line, ms^{-1}) and θ (dashed line, K) valid at **a**, **b** 0000 UTC 27 November 1988, and **c**, **d** 1200 UTC 24 January 1990

of interest. The event case 200 hPa NWS analysis (Fig. 1a) depicts an area of strong wind over the Gulf Coast region, which is a reflection of a subtropical jet streak. Also, the observation-derived cross section (Fig. 1b) clearly depicts the PJ and the STJ. There is subgeostrophic wind over the TX, LA and MS coast (wind barbs crossing the isobars towards lower pressure) indicating a jet streak entrance region. Associated with a jet entrance region is a thermally direct ageostrophic circulation, an area of upper-level divergence and ascent over the Gulf Coast. The supergeostrophic wind (wind barbs crossing the isobars toward higher pressure) over the Carolina Coast indicates the presence of a jet streak exit region. The non-event case 200 hPa NWS analysis (Fig. 1c) depicts a strong PJ extending from northern TX to the northeast US. The observation-derived cross section (Fig. 1d) depicts only a PJ. There is supergeostrophic wind over the TX coast, LA, MS and AL indicating the wind is decelerating, converging and descending. In the event case, there is upper-level divergence, which facilitates ascent while the non-event case has upper-level convergence and sinking over the western Gulf Coast. In the event case, the radar summary (Fig. 2a) depicts strong convection with maximum tops near 16 km over LA and MS. In the non-event

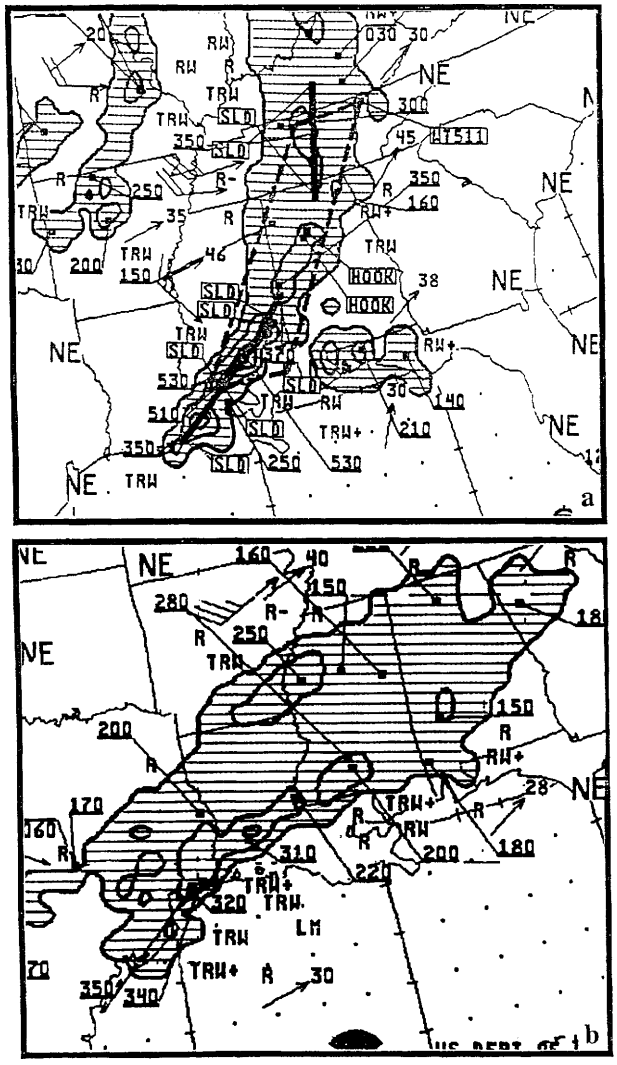

Fig. 2. NWS radar summaries valid at **a** 0035 UTC 27 November 1988, and **b** 1235 UTC 24 January 1990

case, the convection is much less intense with maximum tops near 11 km (Fig. 2b). Also, the non-event case radar summary valid 0035 UTC 25 January 1990 is examined (to consider the effect of daytime heating) and the maximum tops were even lower (9.5 km). This upper-level divergence or convergence directly relates to the strength (depth) of convection.

3.1.2 Event case and non-event case model simulated data

Figure 3 depicts the 200 hPa environment valid at 0000 UTC 27 November 1988 and 1200 UTC 24 January 1990 which corresponds with the NWS analysis above. The event case 200 hPa analyses (Fig. 3a, c) depict an area of strong wind and subgeostrophy over the Gulf Coast region. Over the TX and LA coast, the ageostrophic wind is directed to the northwest indicating upper-level divergence. The 200 hPa subgeostrophy, northwest directed ageostrophic wind and upper-level divergence area corresponds well with the surface convection and is consistent over the entire simulation. The non-event case (Fig. 3b) is very different from the event case. There is a strong PJ over central TX and extending northeast with supergeostrophic wind over the Gulf Coast. Over the LA, MS, AL and FL coast, the southeastward directed ageostrophic wind (Fig. 3d) indicates upper-level convergence over the western Gulf Coast area. The 200 hPa supergeostrophy, southeastward directed ageostrophic wind and upper-level convergence area remains over the Gulf Coast over the entire simulation. The intensity and coverage of upper-level convergence increases with time. In summary, in the event case there is upper-level divergence and ascent, while the non-event case has upper-level convergence and sinking over the western Gulf Coast.

In the event case, convection is associated with a surface trough over eastern TX and western LA early on 26 November 1988. We investigate the upper-level circulations to determine if they are conducive to deep convection. Figure 4 depicts a cross section near the TX/LA border valid 1500 UTC 26 November 1988. The approaching PJ entrance region has an associated thermally direct ageostrophic circulation depicted by the ageostrophic wind vectors. Associated with the circulation is an area of mid- and upper-level divergence (Fig. 4b). Strong ascent (Fig. 4a) and surface convergence is associated with the surface trough (Fig. 16a) and convection (Fig. 16c). By 0000 UTC 27 November 1988 the STJ is over the Gulf Coast States. The NWS analysis (Fig. 1a) depicts the STJ exit region, with supergeostrophic wind, over AL, GA and SC while over western TN the wind associated with the PJ is subgeostrophic. Figure 5 depicts cross sections over TN and AL bisecting both jet streaks. The cross sections depict both the thermally direct circulation associated with the PJ entrance region and the thermally indirect circulation associated with the STJ exit region. Additionally, there is an area of enhanced ascent and upper-level divergence between these jet streaks. Since these features

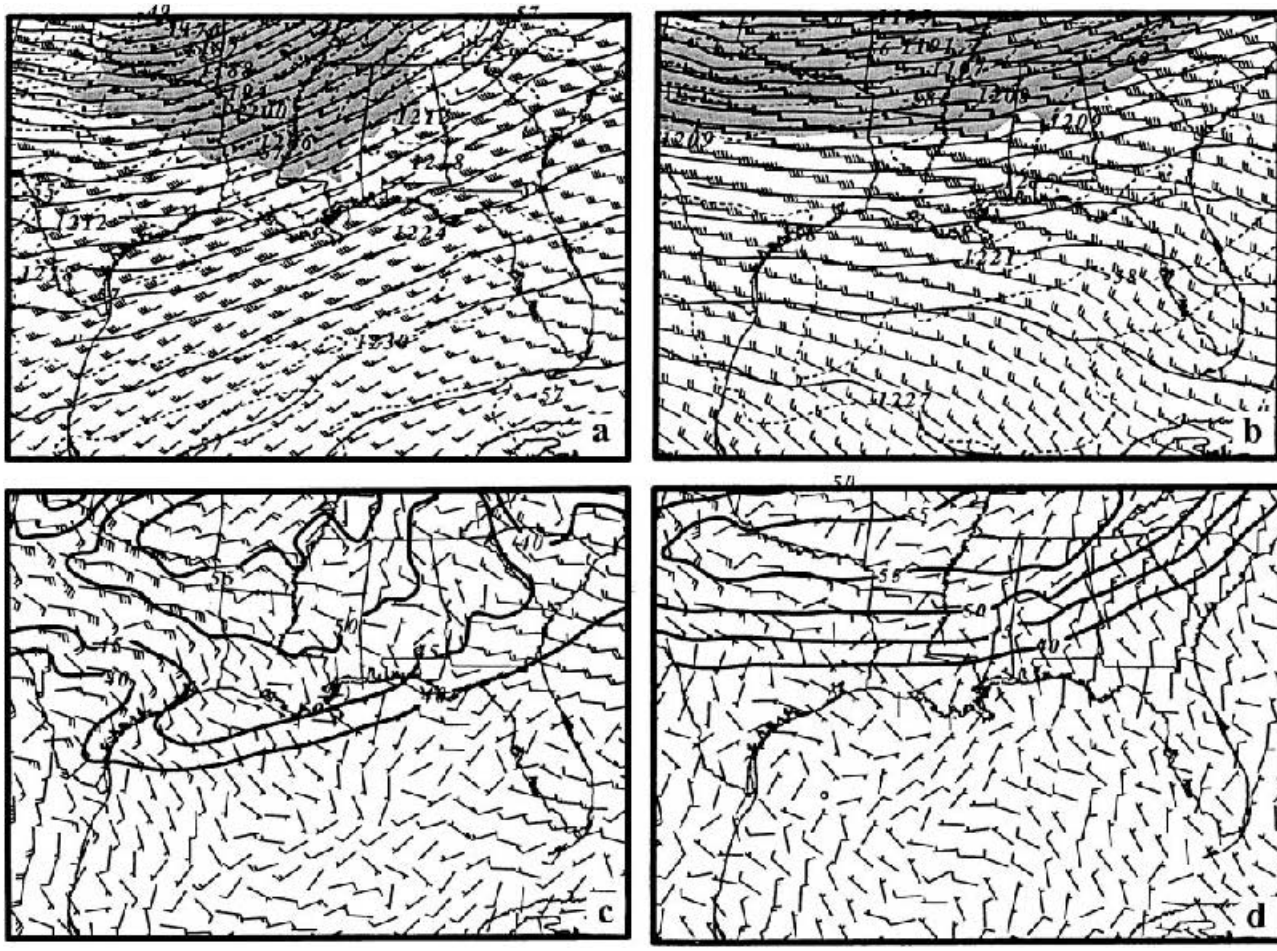

Fig. 3. MASS simulated, 24 km mesh, 200 hPa **a** wind vectors and isotachs (shaded at intervals of 5 for speeds greater than 50), temperature (dashed lines, C), and height (solid lines, dm) and **c** isotachs (contoured at intervals of 5 for speeds greater than 40, ms^{-1}) and ageostrophic wind vectors valid at 0000 UTC 27 November 1988; **b**, **d**, are the same as **a** and **c** but valid at 1200 UTC 24 January 1990

are associated with long lasting jet steaks they are also long lasting and thus facilitate the continuous regeneration of the surface trough and convection. The non-event case analysis (Fig. 1b) depicts supergeostrophic wind over of the Gulf States, which indicates upper-level convergence and descent. Figure 4 depicts cross sections aligned north/south along the TX/LA border valid (0300 UTC 24 January 1990) as the same relative time as the event case. There is very little upper-level divergence and no organized ascent through these levels. Additionally, the downstream cross sections valid 1200 UTC 24 January 1990 (Fig. 5c, d) are also very benign throgh the mid and upper levels. In summary, the jet streaks and associated ageostrophic circulations create mid- and upper-level ascent and divergence thus assisting in the maintenance of the surface trough and production of deep convection in the event case, while these features are absent in the non-event cases.

We examine how the jet streaks modify the environment by comparing the lifted indices (LI) over the Gulf Coast (Fig. 6). For the event case (Fig. 6a), the LI pattern at 1800 UTC 26 November 1988 depicts large negative LI over LA, AR, MS and AL (east of the surface trough and in the warm Mexican airmass), which indicates great potential for severe weather. The non-event case LI field at 0600 UTC 24 January 1990 (Fig. 6b) depicts large positive LI over the Gulf Coast, which indicates little chance for severe weather. We also examined the LI at 1800 UTC to account for solar heating (not shown). The LI values along the Gulf Coast range from 8 to 20, which again indicates little chance for severe weather.

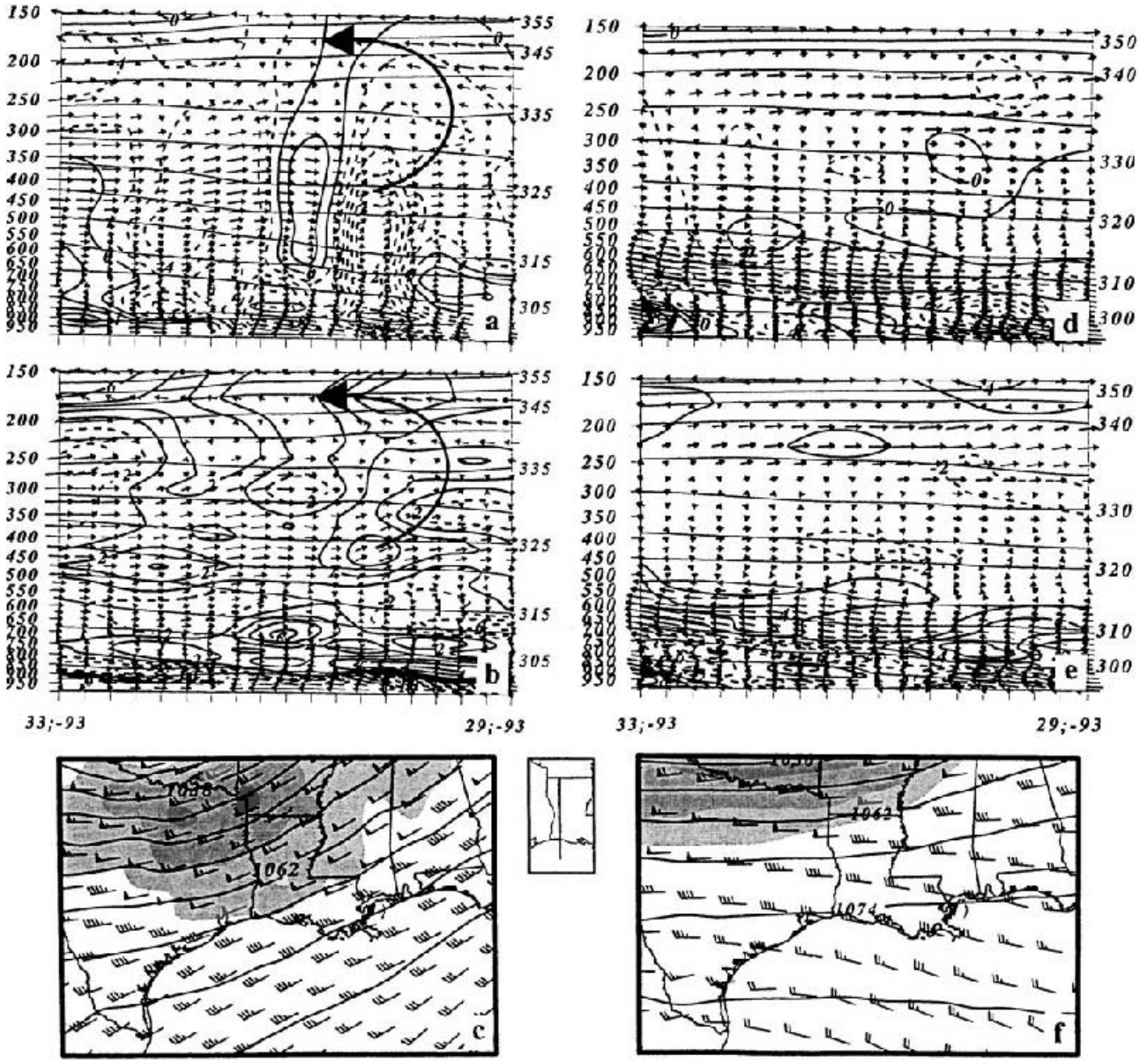

Fig. 4. MASS simulated, 24 km mesh, cross section extending from 33N, 93W to 29N, 93W. Thick arrows represent the structure of the transverse ageostrophic circulations. Includes ageostrophic wind vectors, θ (thin solid lines, K); **a** vertical velocity (contoured every 2 μbs^{-1}, solid lines indicate descent and dashed lines indicate ascent), **b** divergence (contoured every 2×10^{-5} s^{-1}, solid lines positive values and dashed lines negative values) and **c** 250 hPa wind isotach (shaded at intervals of 10 for speeds greater than 50), and vectors, and height (solid lines, dm) valid at 1500 UTC 26 November 1988; **d–f** are the same as **a–c** but valid at 0300 UTC 24 January 1990

Three-dimensional parcel trajectories are constructed to illustrate the forced adjustments imposed upon air parcels as they move through the upper-level jet over LA. First, we examine the event case (Fig. 7a, Table 1). As the parcel moves over eastern TX and LA, it moves through an area of strong upper-level divergence and ascent, which removes mass from the air column and maintains the low-level tough. The trajectory data support the results and conclusion above. The non-event trajectory is depicted in Table 2 and Fig. 7b. The parcel accelerates and ascends slowly along its trajectory. Most notably, the parcel goes through a large area of upper-level convergence, which inhibits any large-scale removal of mass from the air column.

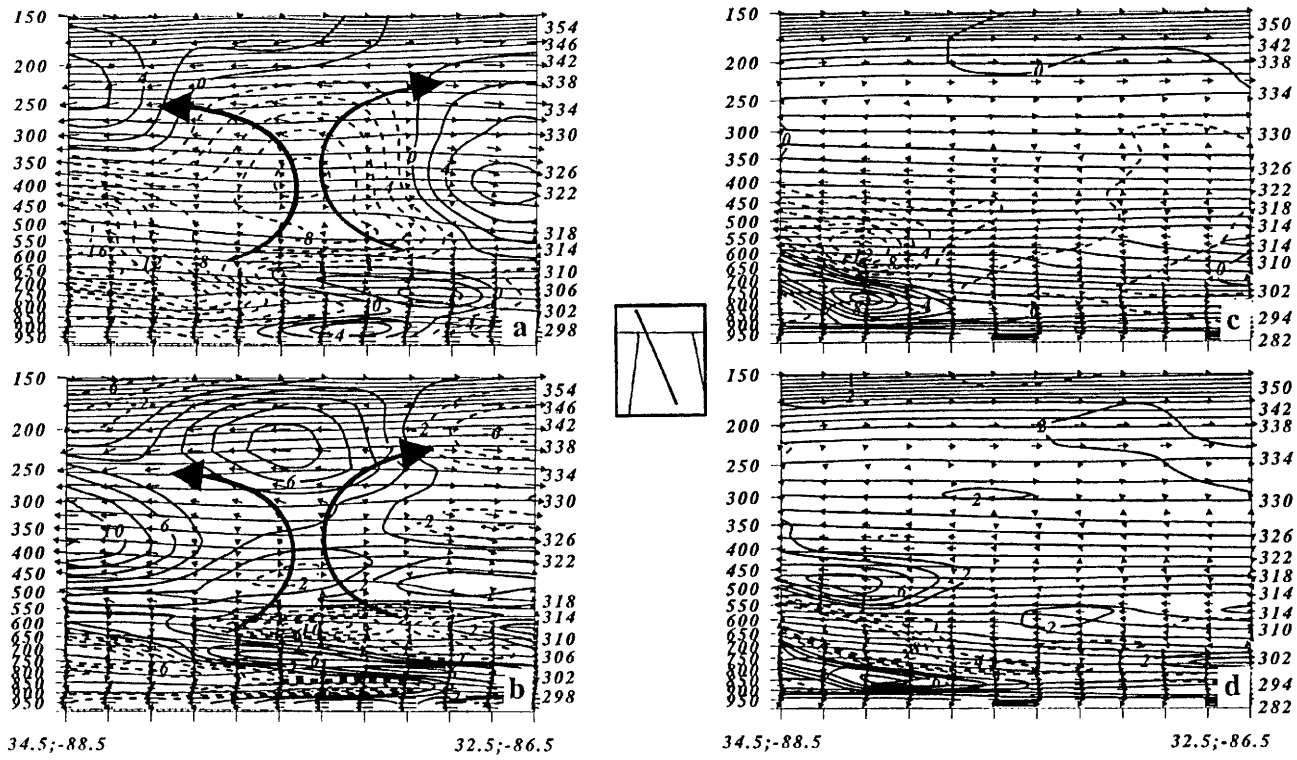

Fig. 5. MASS simulated, 24 km mesh, cross section extending from 34.5N, 88.5W to 32.5N, 86.5W. Thick arrows represent the structure of the transverse ageostrophic circulations. Includes ageostrophic wind vectors, θ (thin solid lines, K); **a** vertical velocity (contoured every 2 μbs^{-1}, solid lines indicate descent and dashed lines indicate ascent) and **b** divergence (contoured every 2×10^{-5} s^{-1}, solid lines positive values and dashed lines negative values) valid at 0000 UTC 27 November 1988; **c** and **d** are the same as **a** and **b** but valid at 1200 UTC 24 January 1990

3.2 Mid-level jet development

In this paper, the mid-level jet is defined by winds greater than 35 ms^{-1} and it is centered about the 600 hPa level. In the event case, a northeastward direceted mid-level jet develops over TX and propagates eastward across the southern states, from TX to GA. In the non-event case, there are two distinct mid-level jets covering two time periods. First, until approximately 2100 UTC 24 January 1990, a thin mid-level jet extends from northern AR to southern TN. Second, after 2100 UTC 24 January 1990 a mid-level jet develops with the low pressure system located to the west of the Appalachians.

3.2.1 Developing thermal and pressure gradients

In the event case, the mid-level jet develops, in large part, due to warm air transported from the Mexican plateau. Figure 8a depicts the warm air moving from the Mexican plateau and over the northwestern Gulf at 1200 UTC 26 November 1988. The 15 °C isotherm (shaded >15) is over eastern TX and just south of the Gulf Coast. The airmass over most portions of the Gulf is in excess of 17 °C. Over the next 24 hours, the warm Mexican air moves eastward over the Gulf States. The sensible heating at the 850 hPa level is essentially zero. Figure 8c valid 0600 27 November 1988 depicts the 15 °C isotherm over central MS and AL. The 0000 UTC 28 November 1988 NWS analysis (not shown) depicts the 15 °C isotherm over eastern NC with Charleston, SC reporting 16 °C. The non-event case, depicted in Fig. 8b valid 0000 UTC 24 January 1990, is very different from the event case. The flow is directed upslope or parallel to the Sierra Madre Mountains thus the warm air remains over the plateau. Figure 8d valid 0000 UTC 25 January 1990 depicts the 15 °C air over the western Gulf and the air over the Gulf Coast States is about 3–4 °C colder than the event case.

The event case jet develops rapidly over central TX between 0900 and 1800 UTC 26 November 1988 (Figs. 9a, b). The development corresponds

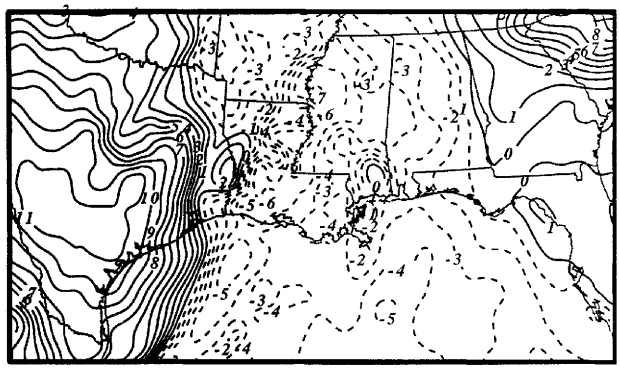

a

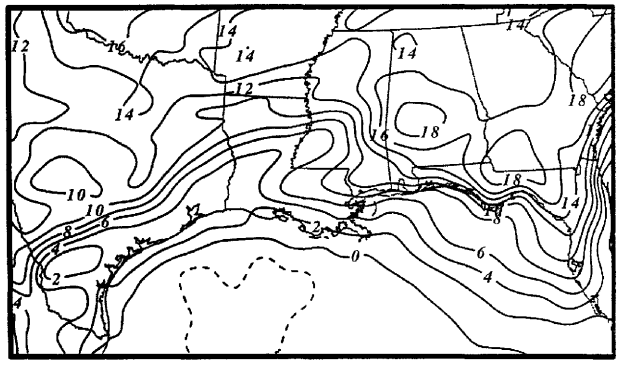

b

Fig. 6. MASS simulated, 24 km mesh, Lifted Index values (solid lines denote positive values and dashed lines denote negative values) valid at **a** 1800 UTC 26 November 1988 and **b** 0600 UTC 24 January 1990

with the increasing 600 hPa thermal and height gradient associated with the eastward moving trough. The thermal gradient and the PGF increase over central LA. At 0900 UTC the magnitude of thermal gradient is about 1 °C/100 km and the PGF per unit mass is 1.9×10^{-3} ms^{-2} and by 1800 UTC the thermal gradient increases to 2.5 °C/100 km and the PGF per unit mass is 3.9×10^{-3} ms^{-2}. At the same time, the wind speed increases from 25 ms^{-1} to 41 ms^{-1}.

The 850 and 700 hPa level temperature change over the 0900 to 1800 UTC time periods are examined (not shown) to measure how the warm MX air effects jet development. At the 700 and 850 hPa levels, north of the jetogenesis area (near Wichita Falls) the temperatures decrease by 4 and 6 °C, respectively. South of the jetogenesis area (near Houston) the 700 and 850 hPa, the temperatures decrease 1 and 0 °C, respectively, The low-level cooling (near Wichita Falls) decreases the 600 hPa heights by approximately 40 m (location A in Fig. 9a, b). The Mexican warm airmass maintains the 600 hPa heights over Houston at approximately 4290 m (location B in Fig. 9a, b). So, the warm Mexican plateau airmass over the Gulf Coast sets up an environment favorable for the development of a mid-level jet. The mid-level jet right entrance region is closely associated with the surface trough over TX/LA border and it is well east of the NWS surface front location over central TX. In the right entrance region of a thermally direct ageostrophic circulation there is ascent, which helps maintain the surface trough.

For the non-event case, there are two periods in the early development and propagation of the mid-level jet. First, until approximately 0600 UTC 25 January 1990, there is a narrow mid-level jet (winds greater than 35 ms^{-1}) extending over northern LA, MS, AL and TN. The jet is associated with the surface front, a narrow band of cold air advection and a strong height gradient. Over northern MS, at 2100 UTC 23 January 1990 (Fig. 9c) the thermal gradient is about 2 °C/100 km and the PGF per unit mass is 2.17 ms^{-2}. By 0600 UTC 24 January 1990 the thermal gradient is about 4 °C/100 km and the PGF per unit mass is 2.92 ms^{-2}. Thus the wind accelerates from 31 ms^{-1} to 36 ms^{-1}. Later, as the cold air advection and its associated thermal, height, and pressure gradients weaken, so does the mid-level jet. By 1800 UTC 24 January 1988 (Fig. 9d) the winds over the coastal states decrease by about 5 ms^{-1}. Second, after 0600 UTC 25 January 1990, a strong mid-level jet develops over the TN Valley in conjunction with a developing QG front/trough system over the Midwest US. Over western TN, at 0300 UTC 25 January 1990, the PGF per unit mass is 1.12×10^{-3} ms^{-2} and by 1800 UTC 25 January 1990, the PGF per unit mass is 4.99×10^{-3} ms^{-2}. Thus, the wind increases from 24 ms^{-1} to 53 ms^{-1}.

The low-level mass and momentum adjustments can be related by examining Fig. 10. In the event case, the transport of the warm Mexican airmass increases the PGF and the mid-level jet. Figures 10a and c, valid 1800 UTC 26 and 27 November 1988, respectively, depict the equivalent potential temperature (Θ_e) of the Mexican airmass defined here as >330 °K. At 1800 UTC 26 November 1988, the warm air originates over the Mexican plateau and extends over the western Gulf to the southeast US. The largest PGF and the

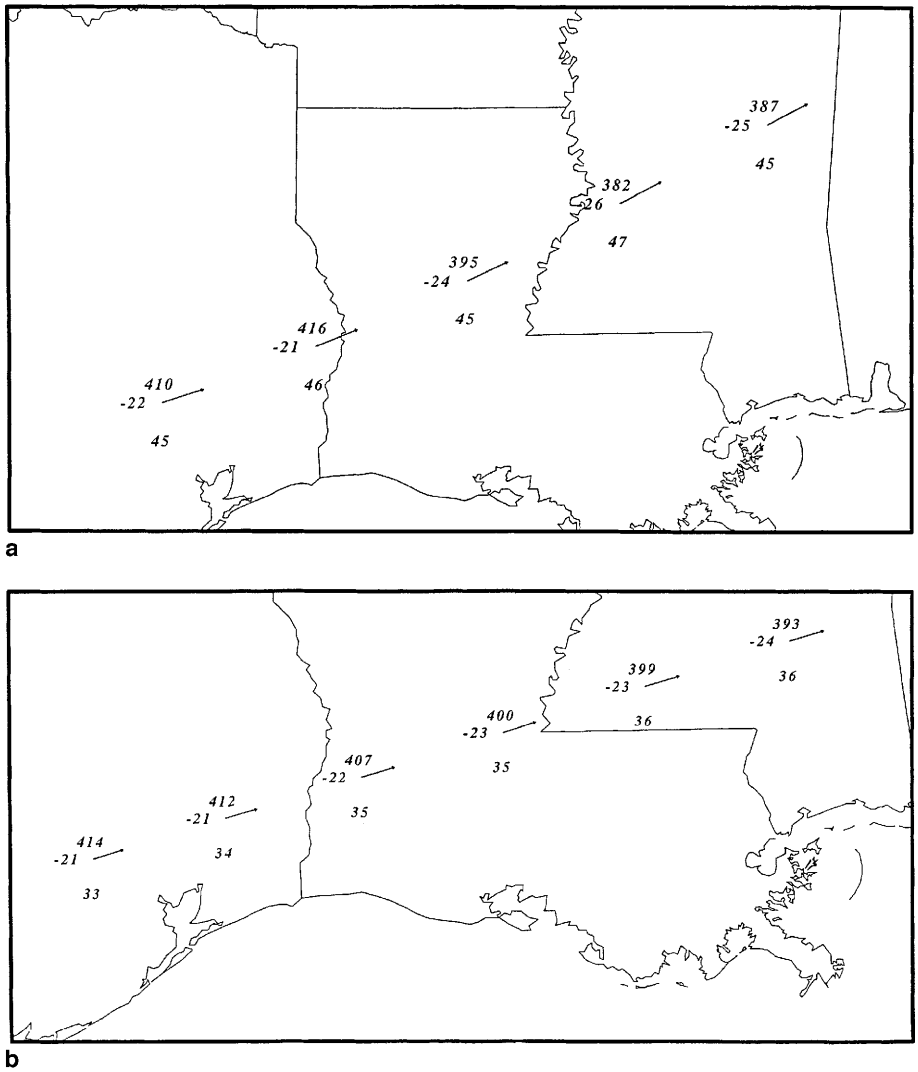

Fig. 7. Trajectories constructed from the 24 km MASS simulations. Station plots contain pressure (hPa), temperature (C), and total wind speed (ms^{-1}). Displayed wind vectors depict total wind; **a** Parcels initialized at 1600 UTC and ended 2000 UTC 26 November 1988; **b** Parcels initialized at 0400 UTC and ended 0800 UTC 24 January 1990

Table 1. Forward trajectory initiated at 1600 UTC 26 November 1988 and ending at 2000 UTC 26 November 1988. Trajectory data is derived from 24 km full physics MASS model run. The following abbreviations are defined: Latitude (LAT), Longitude (LON), Pressure (PRS), Total Wind (V_t), Divergence (DIV), and Omega (OMG)

Time UTC	LAT (°N)	LON (°W)	PRS (hPa)	V_{total} (ms^{-1}) spd/dir	DIV ($\times 10^{-5}$ s^{-1})	OMG (10^{-1} Pa s^{-1})
26/1600	30.4	95.4	410	45.1/251	2.86	4.18
26/1700	30.9	93.8	416	45.2/247	4.59	−3.182
26/1800	31.5	92.2	395	45.4/245	10.9	−17.6
26/1900	32.2	90.6	381	46.5/243	3.25	−0.96
26/2000	32.8	99.6	387	45.4/244	−0.93	5.08

mid-level jet is located on the northwest boundary of this airmass, in the 310 to 320 °K (Θ_e) range. By 1800 UTC 27 November 1988 the warm airmass moves over to SC and GA. Figure 10b, d are cross sections through the jet entrance region. Notice how the warm air is to the southeast of the jet. In the event case the mid-level jet is associated with the warm Mexican airmass over the Gulf Coast. The right entrance region of the jet with its thermally direct circulation and ascent is associated with the surface trough. In the non-event (Fig. 10e, g), valid 0900 UTC 24 and 25 January 1990, the warm Mexican air remains over the plateau. There is a relatively cool pool of air over

Table 2. Same as Table 1 except trajectory initiated at 0400 UTC 24 January 1990 and ending at 0800 UTC 24 January 1990

Time UTC	LAT (°N)	LON (°W)	PRS (hPa)	V_{total} (ms^{-1}) spd/dir	DIV ($\times 10^{-5}$ s^{-1})	OMG (10^{-1} Pa s^{-1})
24/0400	30.4	94.5	412	34/253	−4.432	−1.357
24/0500	30.7	93.2	407	35/253	−4.191	−1.591
24/0600	31.0	92.0	400	35/253	−2.685	−1.069
24/0700	31.3	90.7	399	36/254	−2.178	−0.136
24/0800	31.6	89.4	393	36/255	−1.070	−1.877

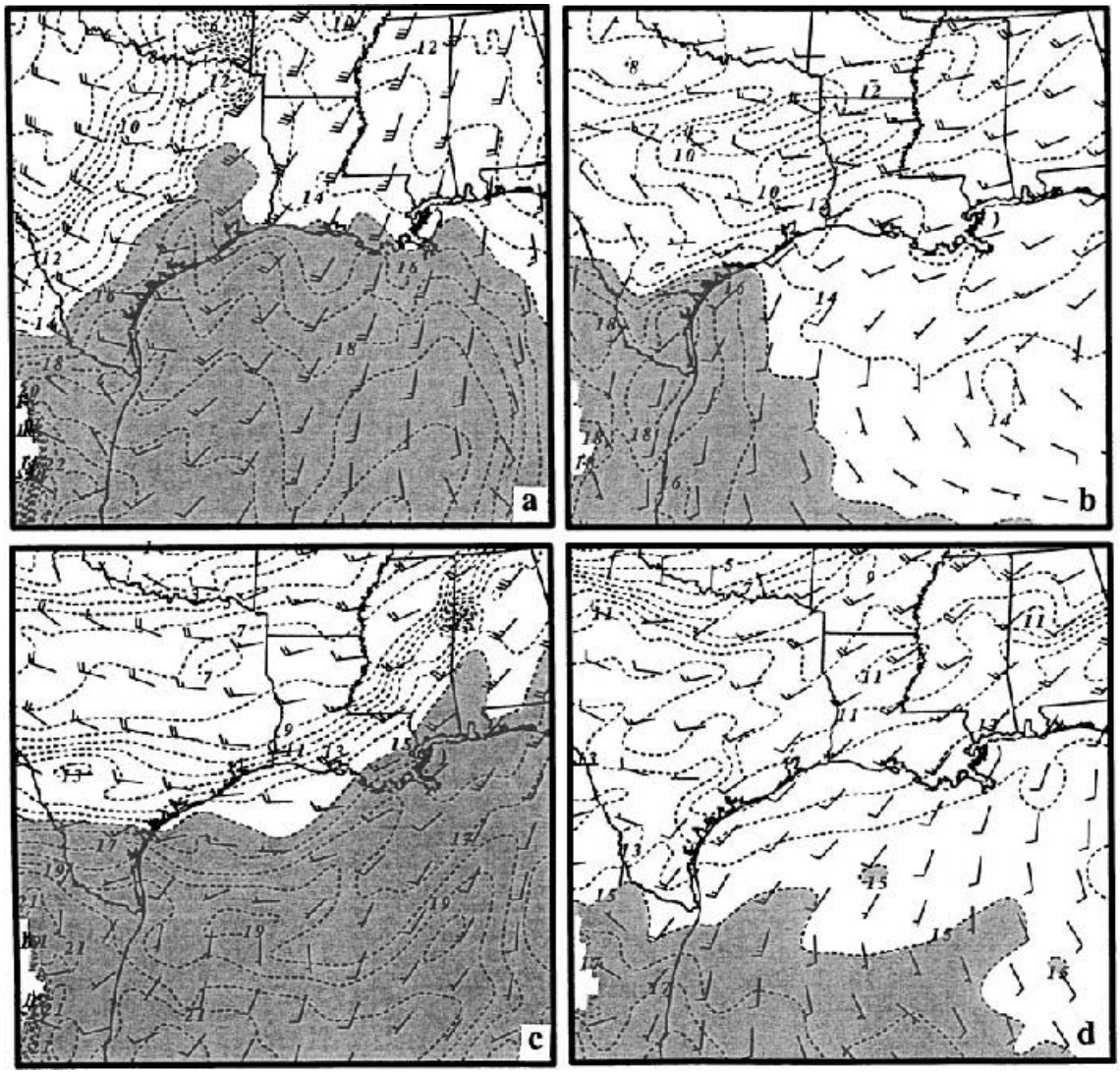

Fig. 8. MASS simulated, 24 km mesh, 850 hPa wind vectors (ms^{-1}) and temperature (dashed lines, (C) and shaded greater than 15) valid at **a** 1200 UTC 26 November 1988, **b** 0000 UTC 24 January 1990, **c** 0600 UTC 27 November 1988, and **d** 0000 UTC 25 January 1990

the western Gulf inhibiting the development of a mid-level jet. The cold air advection over OK, AR and TN increases the PGF and develops a mid-level jet well north of the Gulf.

3.2.2 Three-dimensional trajectory analysis

Three-dimensional parcel trajectories are constructed to illustrate the forced adjustments

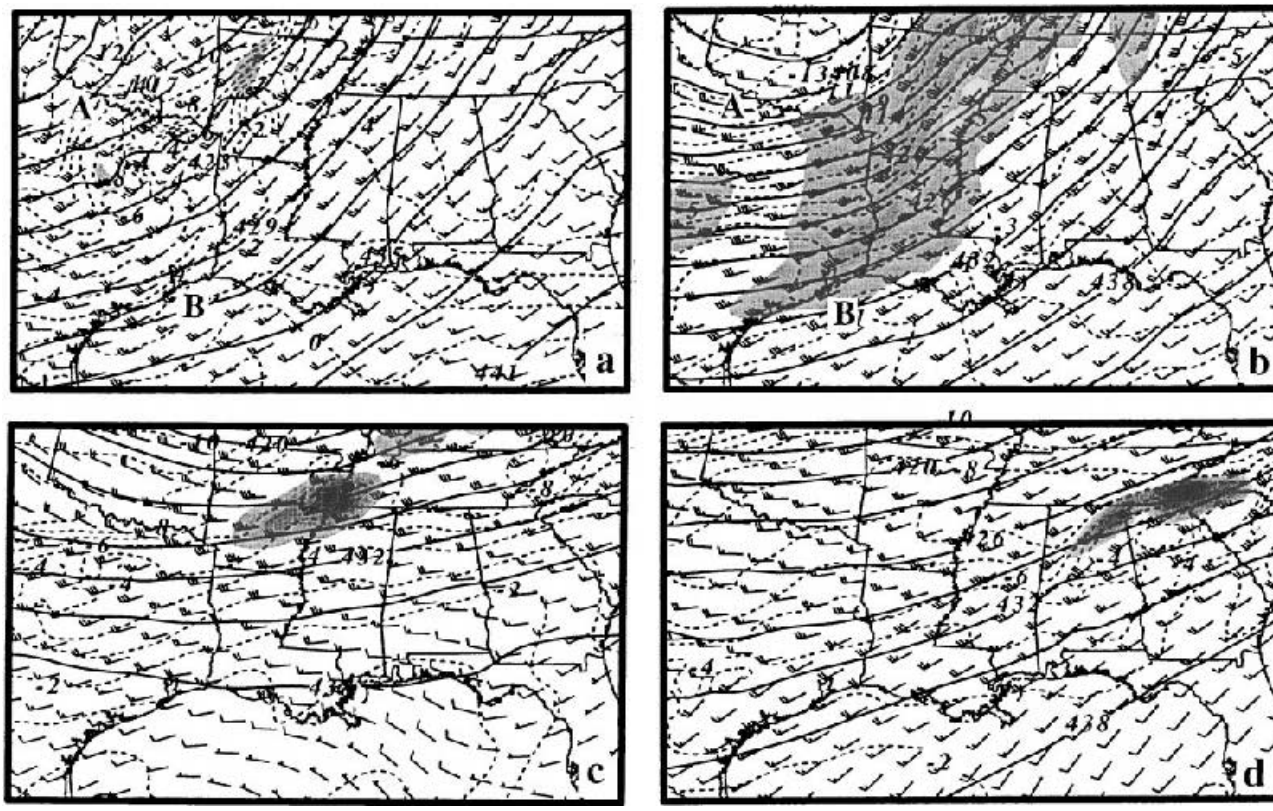

Fig. 9. MASS simulated, 24 km mesh, 600 hPa, wind vectors and isotachs (shaded at intervals of 5 for speeds greater than 35), temperature (dashed lines, C), and height (solid lines, dm) valid at **a** 0900 UTC, **b** 1800 UTC 26 November 1988, **c** 21 UTC 23, and **d** 1800 UTC 24 January 1990. A denotes an area northwest of the jetogenesis area and B denotes an area southeast of the jetogenesis area

imposed upon the air parcels as they move through or near the mid-level jetogenesis region. The event case parcel trajectory (1200 to 1900 UTC 26 November 1988) is depicted in Fig. 11a and Table 3. The parcel originates near the 700 hPa level, moves over the surface trough (and associated convection) near the TX/LA border, ascends rapidly, and ends in the mid-levels over MS. Through 1500 UTC the PGF and the Coriolis force are almost balanced, so the parcel accelerates slightly. The average magnitude difference between the environment PGF and parcel's Coriolis force is $0.19\times10^{-3}\,\mathrm{ms}^{-2}$. Between 1600 to 1900 UTC the parcel moves over the surface trough and into the convection area and ascends rapidly (from 653 to 595 hPa); at this time, the trajectory can be related to Fig. 10a, which depicts the 600 hPa jet. The environmental PGF is much stronger than the parcel's associated Coriolis force, which accelerates the parcel. As the parcel ascends it accelerates due to the increasing magnitude difference between the PGF and Coriolis force, which increases from $0.16\times10^{-3}\,\mathrm{ms}^{-2}$ (1500 UTC) to $1.71\times10^{-3}\,\mathrm{ms}^{-2}$ (1800 UTC). Also, the 700 hPa level height contours are orientated more north-south than the 500 hPa isobars (the lower-level parcels have more southerly momentum). When the parcel (originating from the 700 hPa level) is ejected near the 500 hPa level it carries with it more southerly momentum. Thus, the parcel at its new higher level crosses the isobars toward lower pressure and accelerates.

The mid-level parcel trajectory of the non-event case (0000 to 0900 UTC 24 January 1990) is depicted in Fig. 11b and Table 4. Table 4 lists the parcel's accelerations as it moves over the Gulf Coast States. Again, the trajectory can be related to Fig. 10c; at this time there is no 600 hPa jet near the Gulf Coast. Initially, the air parcel accelerates because it is in an area of subgeostrophy. In this case, there is less southerly momentum than the event case. Over the TX coast, trajectories of both the event and non-

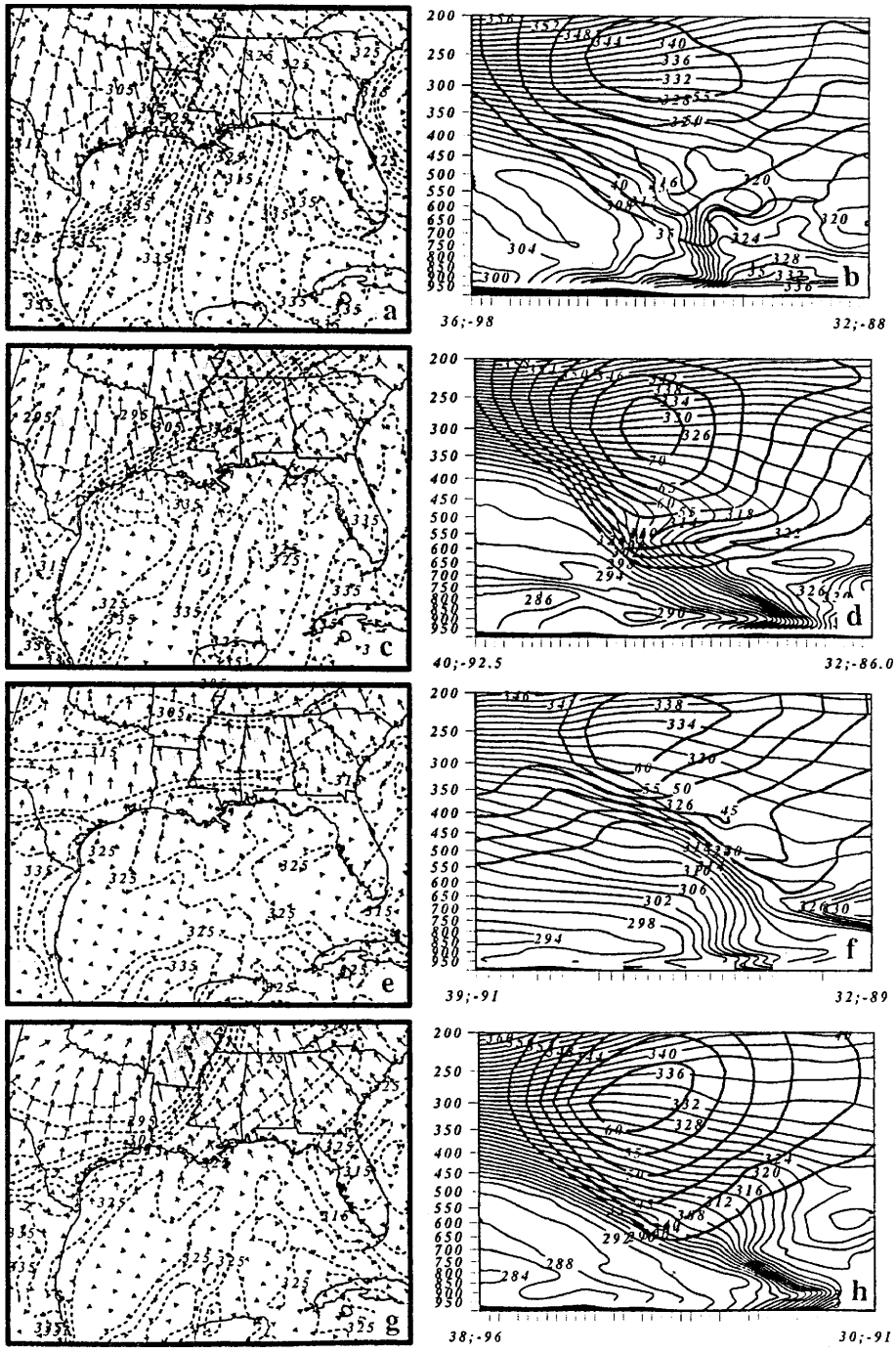

Fig. 10. MASS simulated, 24 km mesh, 600 hPa, wind isotachs (shaded at intervals of 5 for speeds greater than 35 ms^{-1}), θ_e (dashed lines, K), and pressure gradient force vectors (ms^{-2}). Cross sections include θ_e (thin solid lines, K) and isotachs (thick solid lines, contoured at intervals of 5 for speeds greater than 35 ms^{-1}). Valid at **a** and **b** 1800 UTC 26, **c** and **d** 1800 UTC 27 November 1988, **e** and **f** 0900 UTC 24, **g** and **h** 0900 UTC 25 January 1990

event case are the same, but once they enter LA, the tracks diverge. In the event case, as the parcels ascend (carrying with them the southerly momentum), the track becomes more northward. The non-event case trajectory remains on a easterly path.

3.2.3 Mid-level jet development and convection

We examine the relationship between convection and jet development. If convection is an important forcing mechanism for midlevel jet development, suppressing convection will weaken the jet.

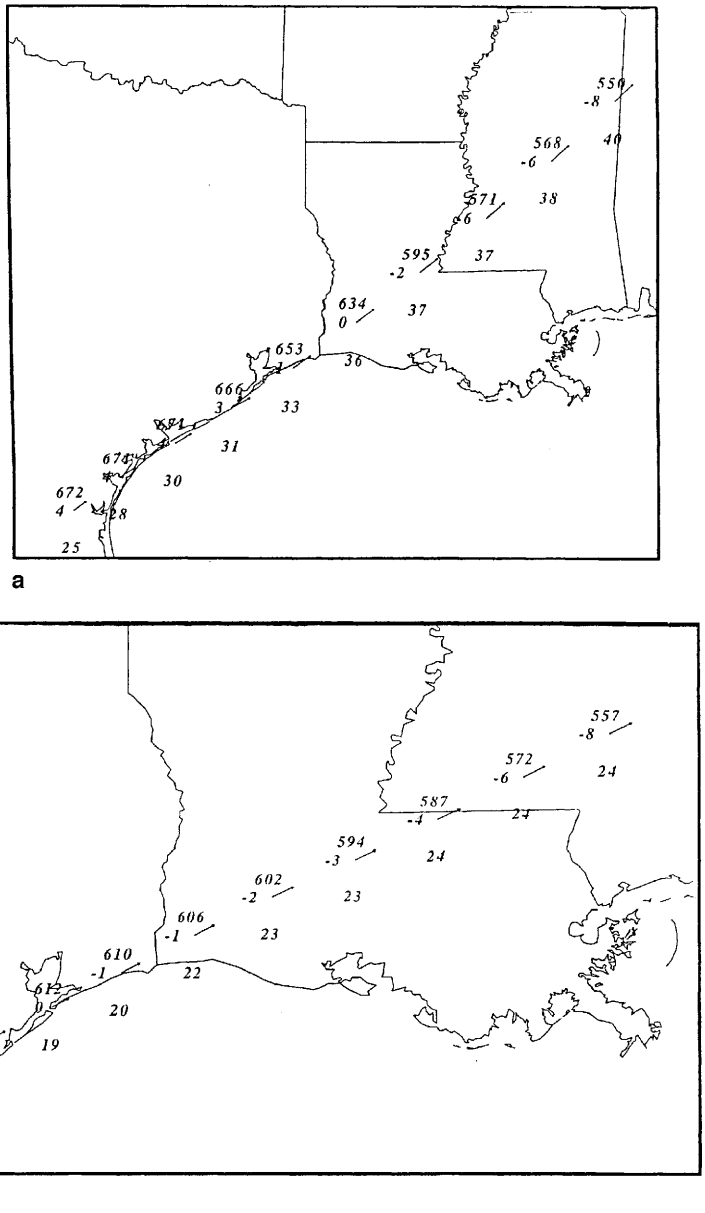

Fig. 11. Trajectories constructed from the 24 km MASS simulations. Station plots include pressure (hPa), temperature (C), and total wind speed (ms^{-1}). Displayed wind vectors depict total wind; **a** parcels initialized at 1200 UTC and ended at 2100 UTC 26 November 1988; **b** parcels initialized at 0100 UTC and ended at 0900 UTC 24 January 1990

Convection (latent heating) warms the local environment, increases the thickness of the air column, inceases the PGF near the middle of the column, which accelerates the jet. In the event case, the convection area is associated with the mid-level jet right entrance region and in the warm MX airmass. In the non-event case, the only area of significant convection is occurring over the coast near the TX/LA border, which is well away from the mid-level jet.

Another MASS simulation is performed surpressing the release of latent heat (convection) to examine the relationship between jet development and convection, In the event case "no latent heat" simulation, a mid-level jet develops by 1800 UTC 26 November 1988 (Fig. 12) over TX and LA with approximately the same wind speed as in the case with latent heating. This supports the idea that the warm, low-level airmass transported from the Mexican plateau maintains the height gradient over the TX/LA border and develops the mid-level jet. The environment is predisposed to produce a mid-level jet. Convection (latent heating) does modify the jet over AR where the wind speeds are 5–10 ms^{-1} higher for the simulation with convection. For the non-event case, the 600 hPa depictions valid 2100 UTC 23 (Fig. 13a) and 0600 24 January 1990 (Fig. 13b) highlight the fact that the

Table 3. Forward trajectory initiated at 1200 UTC 26 November 1988, passing through the mid-level jetogenesis, and ending at 2100 UTC 26 November 1988. Trajectory data is derived from 24 km full physics MASS model run. The following abbreviations are defined: Latitude (LAT), Longitude (LON), Pressure (PRS), Coriolis force vector (CO), Pressure gradient force vector (PGF), Magnitude difference between PGF and CO (PGFCO), Total Wind (V_t), and Omega (OMG)

Time UTC	LAT (°N)	LON (°W)	PRS (hPa)	CO 10^{-3} ms^{-2} spd/dir	PGF 10^{-3} ms^{-2} spd/dir	PGFCO 10^{-3} ms^{-2}	V_{total} (ms^{-1}) spd/dir	OMG 10^{-1}Pa s^{-1}
26/1200	27.5	98	671	1.7/320	1.8/140	0.1	25/230	0.25
26/1300	28.5	97	671	1.93/324	1.73/162	0.2	28/234	−2.47
26/1400	28.8	96	671	2.1/328	2.4/153	0.3	30/238	−0.1
26/1500	29.1	95	666	2.23/328	2.39/166	0.16	31/238	−6.28
26/1600	29.6	94.2	653	2.41/325	3.36/166	0.95	33/235	−1.31
26/1700	30.3	93.2	634	2.68/323	3.81/155	1.13	36/233	−5.32
26/1800	31.1	92	595	2.83/321	4.54/189	1.71	37/231	−33.6
26/1900	31.8	91	571	2.92/320	3.3/143	0.38	37/230	−3.19
26/2000	32.6	89.8	568	3.01/318	3.54/151	0.53	38/228	0.035
26/2100	33.5	88.7	550	3.2/322	3.51/143	0.31	40/227	−15.66

Table 4. Same as Table 3 except trajectory is initiated at 0100 UTC 24 January 1990 and ending 0900 UTC 24 January 1990

Time UTC	LAT (°N)	LON (°W)	PRS (hPa)	CO 10^{-3} ms^{-2} spd/dir	PGF 10^{-3} ms^{-2} spd/dir	PGFCO 10^{-3} ms^{-2}	V_{total} (ms^{-1}) spd/dir	OMG 10^{-1}Pa s^{-1}
24/0100	29.1	95.4	614	1.2/332	1.3/165	0.1	17.4/242	0.124
24/0200	29.4	94.8	612	1.3/333	1.5/171	0.2	18.7/242	0.926
24/0300	29.7	94.1	610	1.4/332	1.5/149	0.1	20.4/242	0.832
24/0400	30.0	93.4	606	1.6/333	1.4/190	−0.2	21.7/243	1.026
24/0500	30.3	92.7	602	1.7/334	1.5/182	−0.2	22.6/244	1.565
24/0600	30.6	91.9	594	1.7/335	1.9/175	0.2	23.4/245	1.975
24/0700	31	91.1	587	1.8/335	1.9/168	0.1	23.8/245	2.768
24/0800	31.3	90.3	572	1.8/335	1.7/162	−0.1	23.9/245	4.847
24/0900	31.6	89.4	557	1.9/335	2.0/137	0.1	24.3/245	10.23

jet locations and intensity are slightly different between these two cases (with and without latent heating). The 600 hPa jet (over LA and MS) is farther to the south, the wind speeds are about 5 ms^{-1} faster and the area of subgeostrophy is farther to the south in the case with latent heating. So, the front and precipitation over MO, IL and KY modifies the mid-level winds over the Gulf Coast States.

Parcel trajectories are constructed for the event case without latent heating (Table 5, Fig. 14). The parcel travels approximately the same path as in the simulation with latent heating supporting the idea that the atmosphere is predisposed to create a mid-level jet with or without the latent heat release. The parcel with latent heating ends at a higher level (550 vs. 583) and slightly faster (40 ms^{-1} vs. 38 ms^{-1}). Since the parcel with the latent heat exits at a higher level, with more southerly momentum, it remains unbalanced and continues to accelerate (Uccellini et al., 1984). In the non-event case, the parcel trajectories are different between the simulations with or without latent heating (Table 6, Fig. 15). The parcel with

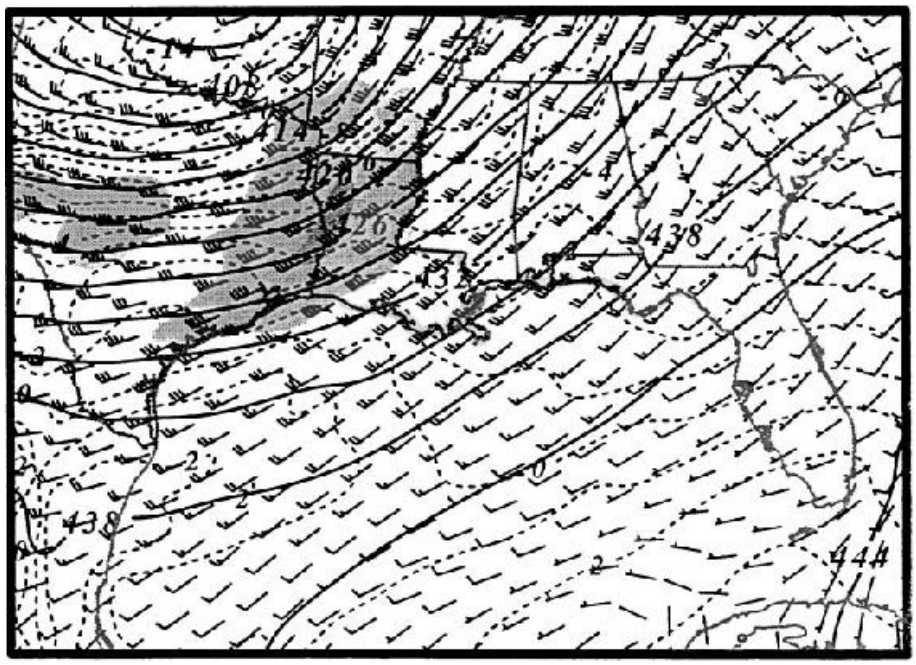

Fig. 12. MASS simulation without latent heating, 24 km mesh, 600 hPa, wind vectors and isotachs (shaded at intervals of 5 for speeds greater than 35), temperature (dashed lines, C), and height (solid lines, dm) valid at 1800 UTC 26 November 1988

latent heating is directed more northward and ends at a higher level (557 vs. 583) and faster (24 ms^{-1} vs. 19 ms^{-1}). So, the frontal system and associated latent heat release over MO, IL and KY creates a slightly stronger mid-level jet over the Gulf Coast.

In summary, in the event case the environment is predisposed to create a mid-level jet due to the warm Mexican air mass transported over the Gulf States. Late in the period, convection enhances the aerial coverage of the mid-level jet over the Gulf Coast. The convection and surface trough over the Gulf Coast are associated with the right entrance region of the jet. The thermally direct ageostrophic circulation about the jet maintains the trough and convection by removing mass from the air column. In the non-event case, latent heating associated with a frontal boundary over MO, IL and KY enhances the mid-level jet north of the Gulf Coast so the ageostrophic circulation (ascent) does not enhance convection along the coast.

4. Surface convergence zone and squall line

Part 1 discussed the differences in the synoptic scale forcing between the cases. In this section, we examine a surface convergence zone and a mid-level jet.

4.1 Surface trough development and propagation.

The model output of the event case compares well with the NWS analysis. At 1500 UTC 26 November 1988 the MASS simulation depicts strong surface confluence over the TX/LA border extending into AR (Fig. 16a). The model depicts a meso-trough associated with the confluence zone. Moist air is to the east of the confluence zone with dry air over central TX. the NWS surface analysis (Fig. 16b) has similar features. The wind pattern is very similar with a confluence zone over the TX/LA border. A surface trough is depicted over eastern TX and a squall line over central AR. Also, the moist air is east of the confluence zone and the dry air is over central TX. Both the radar summary (Fig. 16c) and the simulated convective precipitation field (not shown) indicate that convection occurs in the same areas. The strongest simulated convective precipitation is over the TX/LA border and the convection on the radar summary has the highest cloud tops (~15 km) in that area. For the next 24 hours, the model-

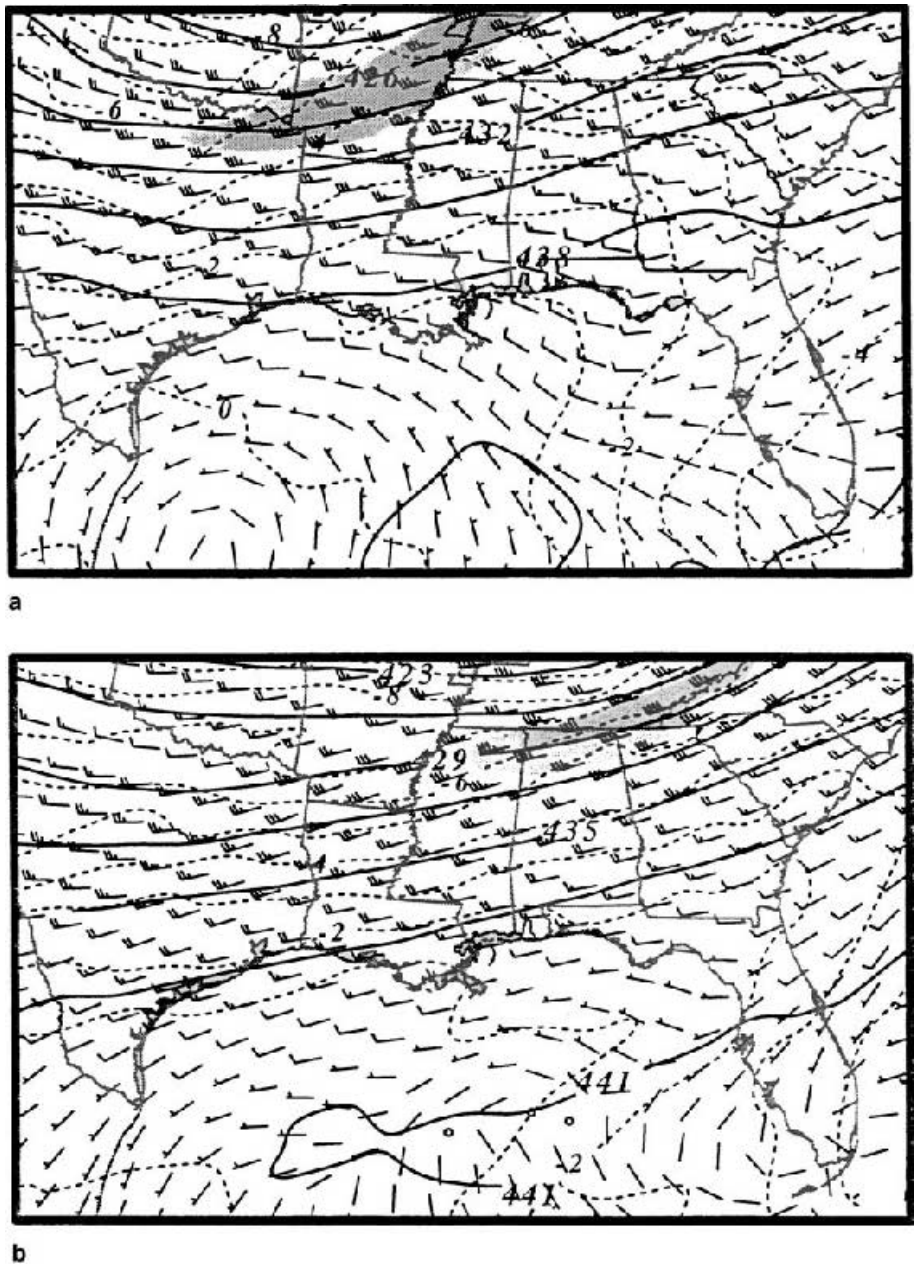

Fig. 13. MASS simulation without latent heating, 24 km mesh, 600 hPa, wind vectors and isotachs (shaded at intervals of 5 for speeds greater than 35), temperature (dashed lines, C), and height (solid lines, dm) valid at **a** 0900 UTC 23 January 1990 and **b** 1800 UTC 23 January 1990

Table 5. Same as Table 3 except the data is derived from 24 km MASS simulation without latent heating

Time UTC	LAT (°N)	LON (°W)	PRS (hPa)	CO 10^{-3} ms^{-2} spd/dir	PGF 10^{-3} ms^{-2} spd/dir	PGFCO 10^{-3} ms^{-2}	V_{total} (ms^{-1}) spd/dir	OMG μb s^{-1}
26/1300	27.3	97.3	637	1.6/319	1.7/187	0.1	23/229	0.457
26/1400	27.8	96.6	635	1.8/322	2.0/171	0.2	27/232	−3.842
26/1500	28.4	95.7	620	2.1/232	2.1/183	0.0	29/232	−3.175
26/1600	29.0	94.8	613	2.3/324	2.3/177	0.0	33/234	−0.368
26/1700	29.6	93.8	609	2.5/325	2.3/148	−0.2	35/235	−3.645
26/1800	30.3	92.7	600	2.7/324	2.8/153	0.1	36/234	−0.786
26/1900	31.0	91.6	592	2.8/323	3.0/154	0.2	37/233	−3.377
26/2000	31.8	90.4	584	2.9/323	3.0/142	0.1	38/233	−2.153
26/2100	34.5	89.3	583	2.9/323	3.0/139	0.1	38/234	−0.479

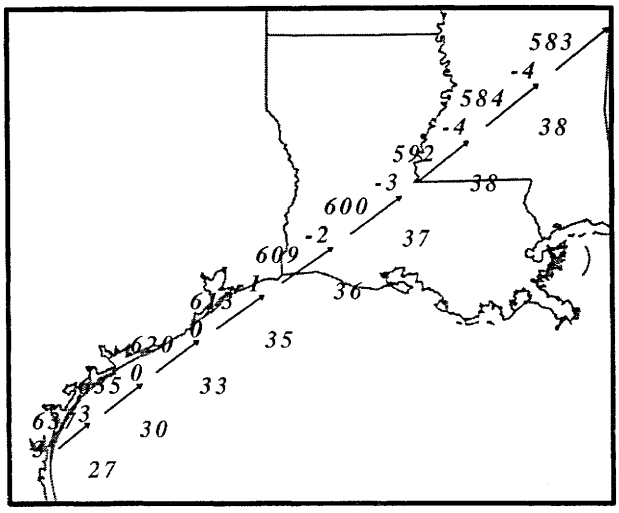

Fig. 14. Trajectory constructed from the 24 km MASS simulation without latent heating. Station plots contain pressure (hPa), temperature (C), and total wind speed (ms^{-1}). Displayed wind vectors depict total wind. Parcels initialized at 1300 UTC and ended 2100 UTC 26 November 1988

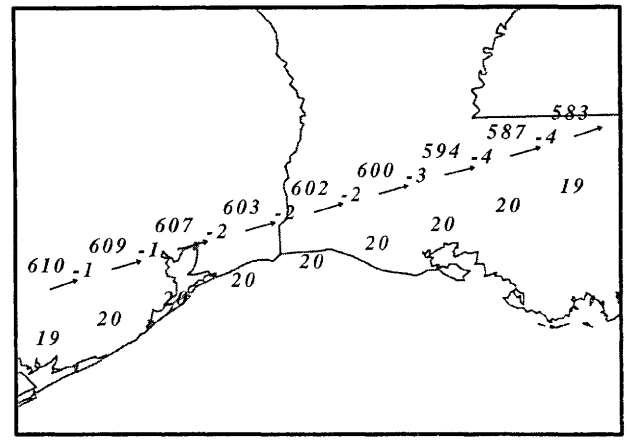

Fig. 15. Trajectory constructed from the 24 km MASS simulation without latent heating. Station plots contain pressure (hPa), temperature (C), and total wind speed (ms^{-1}). Displayed wind vectors depict total wind. Parcels initialized at 0100 UTC and ended 0900 UTC 24 January 1990

simulated surface trough (confluence area) propagates across the Gulf Coast states. At the same time, the NWS analysis modifies the squall line into a trough and by 1200 UTC 27 November 1988 the trough is depicted as a could front (moving over GA and AL).

In the non-event case, the MASS-simulated environment (Fig. 17a) is almost identical to the NWS analysis (Fig. 17b). At the same relative time as the event case (0300 UTC 24 January 1990) there is a quasi-stationary front over the TX/OK border extending across AR, TN and KY. Also, a weak surface frontal system (trough) is moving onshore over the Gulf Coast. The lower atmosphere is much drier than the event case with the only moist air over the Gulf Coast. The only significant convection is over the Gulf Coast at the TX/LA border, as depicted on both the radar summary (Fig. 17c) and the simulated convection field. At this time, there is upper-level convergence over the Gulf Coast, which may inhibit deep convection. In the non-event case, the maximum tops of the convective cells over the Gulf Coast are 6–7 km lower than that of the event case. The NWS analysis depicts the front over the coast as a trough over the next 24 hours then begins to redevelop by 1800 UTC 24 January 1990. The only area of convective precipitation is

Table 6. Same as Table 4 except the data is derived from 24 km MASS simulation without latent heating

Time UTC	LAT (°N)	LON (°W)	PRS (hPa)	CO 10^{-3} ms^{-2} spd/dir	PGF 10^{-3} ms^{-2} spd/dir	PGFCO 10^{-3} ms^{-2}	V_{total} (ms^{-1}) spd/dir	OMG μb s^{-1}
24/0100	29.4	96.3	610	1.4/339	1.3/160	0.1	19/249	−0.358
24/0200	29.6	95.6	609	1.4/343	1.6/158	0.2	20/253	0.482
24/0300	29.8	94.9	607	1.5/344	1.5/159	0.0	20/254	−1.358
24/0400	30.0	94.2	603	1.5/344	1.5/171	0.0	20/254	−0.421
24/0500	30.1	93.4	602	1.5/344	1.5/172	0.0	20/254	0.076
24/0600	30.3	92.7	600	1.5/345	1.6/167	0.1	20/255	−1.426
24/0700	30.5	92	594	1.5/346	1.5/166	0.0	20/256	−2.142
24/0800	30.6	91.3	587	1.5/345	1.4/135	−0.1	20/255	−1.333
24/0900	30.8	90.6	583	1.4/343	1.3/151	−0.1	19/253	−1.062

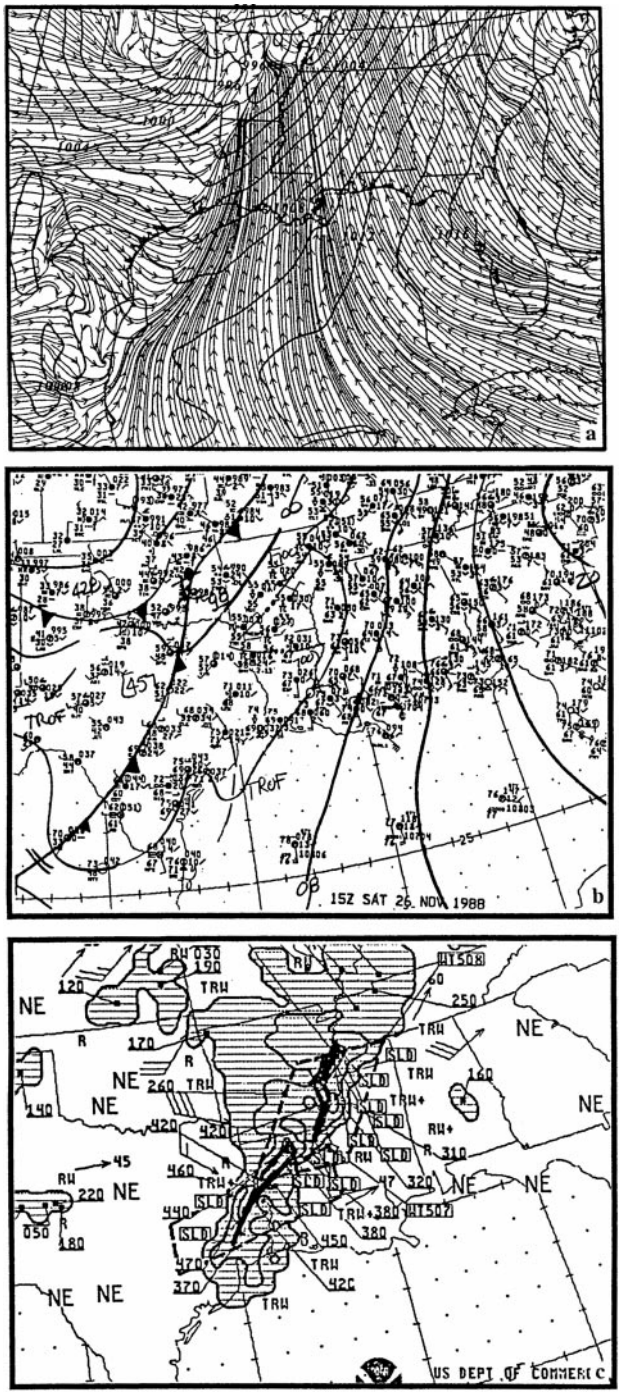

Fig. 16. **a** MASS simulated, 24 km mesh, surface depiction including surface streamlines, mean sea-level pressure (solid lines, hPa), **b** NWS surface analysis, and **c** NWS radar summaries valid at 1500 UTC 26 November 1988

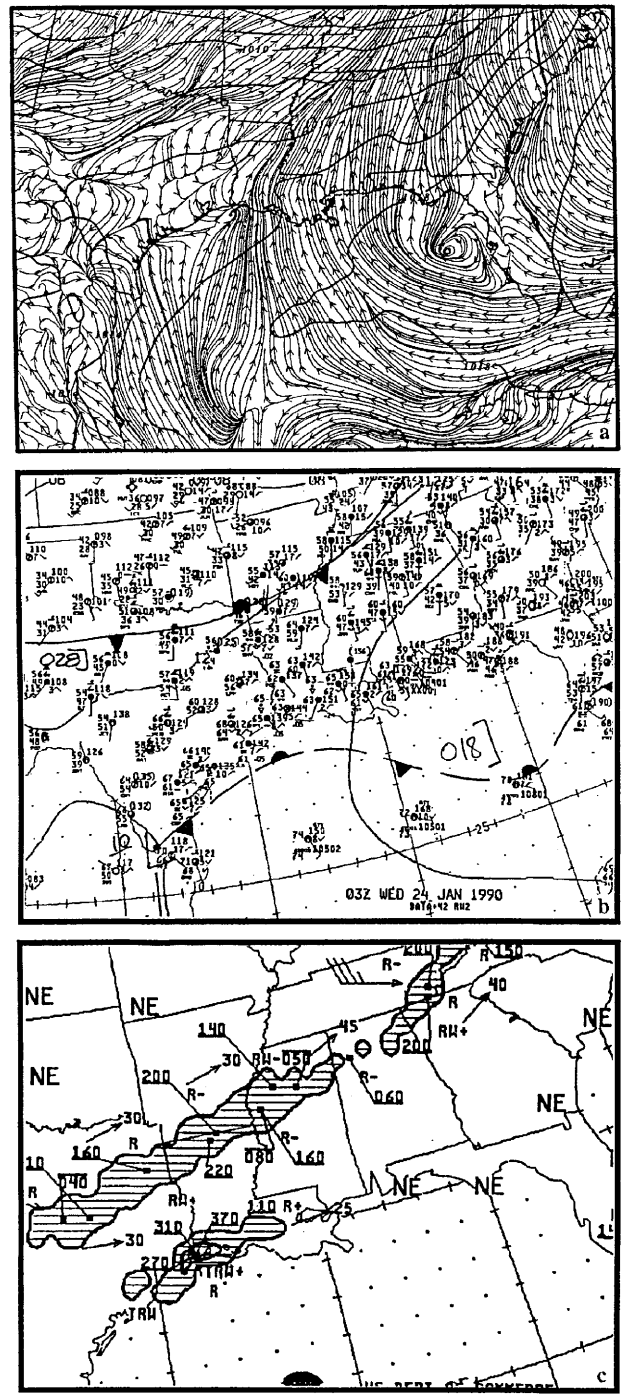

Fig. 17. **a** MASS simulated, 24 km mesh, surface depiction including surface streamlines, mean sea-level pressure (solid lines, hPa), **b** NWS surface analysis, and **c** NWS radar summaries valid at 0300 UTC 24 January 1990

associated with this front/trough over the coast, which increases in coverage and intensity but it is always much less than the event case. The absence of upper-level support (no STJ and the mid- and PJ are well to the north) inhibits deep convection.

4.2 Mid-level jet coupling with low-level forcing

The mid-level jet (600 hPa) is examined to determine if it is coupled to the low-level forcing. At 0600 UTC 26 November 1988 winds over

eastern TX are 20 ms^{-1} and by 2100 UTC 26 November 1988 the jet across eastern TX and central LA accelerates to 40 ms^{-1}. Over eastern TX and LA, the wind is highly subgeostrophic, which accelerates in response to the environment (jet streak entrance region). The accelerating wind field produces an area of mid-level divergence and ascent, which maintains both the surface trough and convection. Figure 18 depicts the vertical environment through the mid-level jetogenesis area and over the surface trough. The low-level convergence and mid- and upper-level divergence facilitate strong ascent up to the 350 hPa level. The surface trough moves in conjunction with the mid-level jet and the upper-level divergence. Figures 19a–c depict the surface trough (confluence zone) and the 600 hPa jet and Figs. 19d–f depict the surface trough (confluence zone) and the 250 hPa divergence valid 1800 UTC 26, 0600 UTC 27 and 1800 UTC 27 November 1988, respectively. The surface trough (confluence zone) is located to the right of the entrance region of the 600 hPa jet and to the left of the upper-level divergence. At 1800 UTC (Fig. 19c), the trough develops into a frontal boundary so the trough covers a much broader area.

In the non-event case, the mid-level jet (600 hPa) is associated with the quasi-stationary front over TX/OK border and over TN (not shown). The mid-level jet is not associated with the area of convection along the Gulf Coast. At 0300 UTC the maximum winds (35 ms^{-1}) are over southern AR and northern MS. Over the next 24 hours, there is little change to the jet location except the maximum wind speeds have moved farther east (over GA). Throughout this mid-period the mid-level jet is not over the Gulf Coast.

In summary, the event case mid-level jet is coupled to the surface trough over the Gulf Coast. Under this situation, the low-level air parcels enter

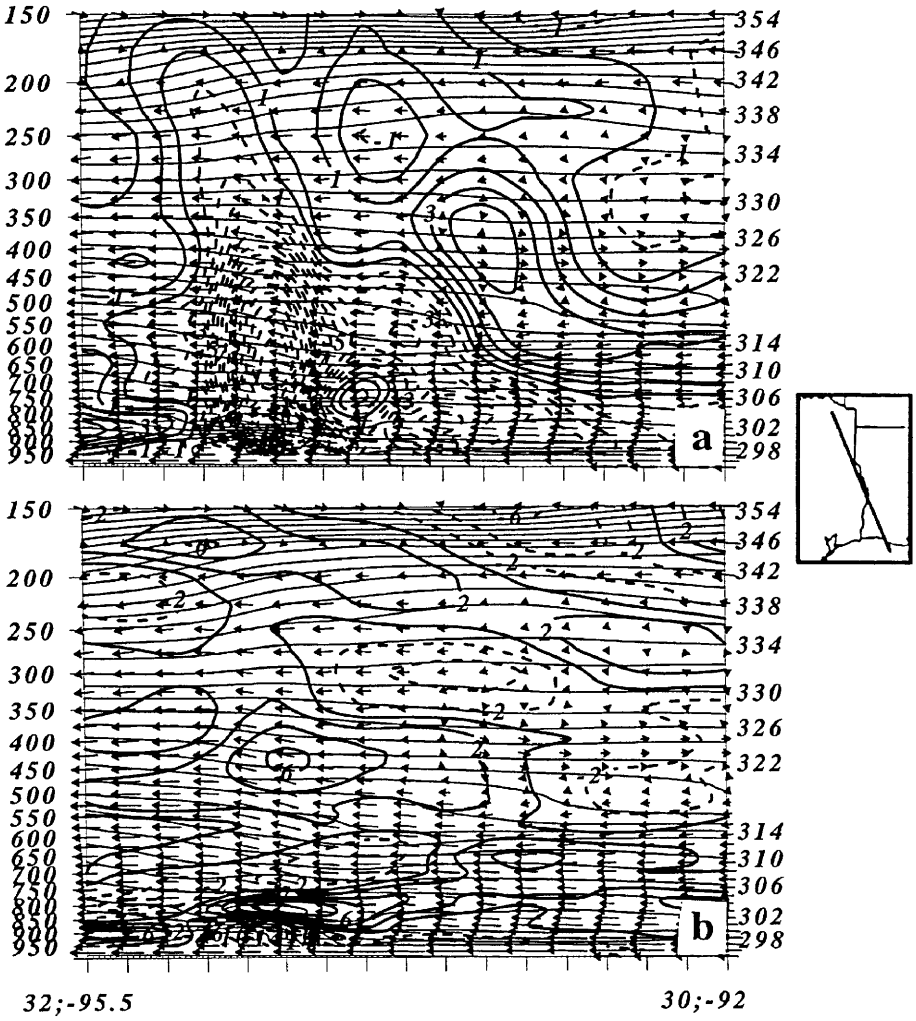

Fig. 18. MASS simulated, 24 km mesh, cross section extending from 32N, 95.5W to 30N, 92W valid at 1500 UTC 26 November 1988. Includes ageostrophic wind vectors, θ (thin solid lines, K), **a** vertical velocity (contoured every 2 μbs^{-1}, solid lines indicate descent and dashed lines indicate ascent), and **b** divergence (contoured every 2×10^{-5} s^{-1}, solid lines positive values and dashed lines negative values)

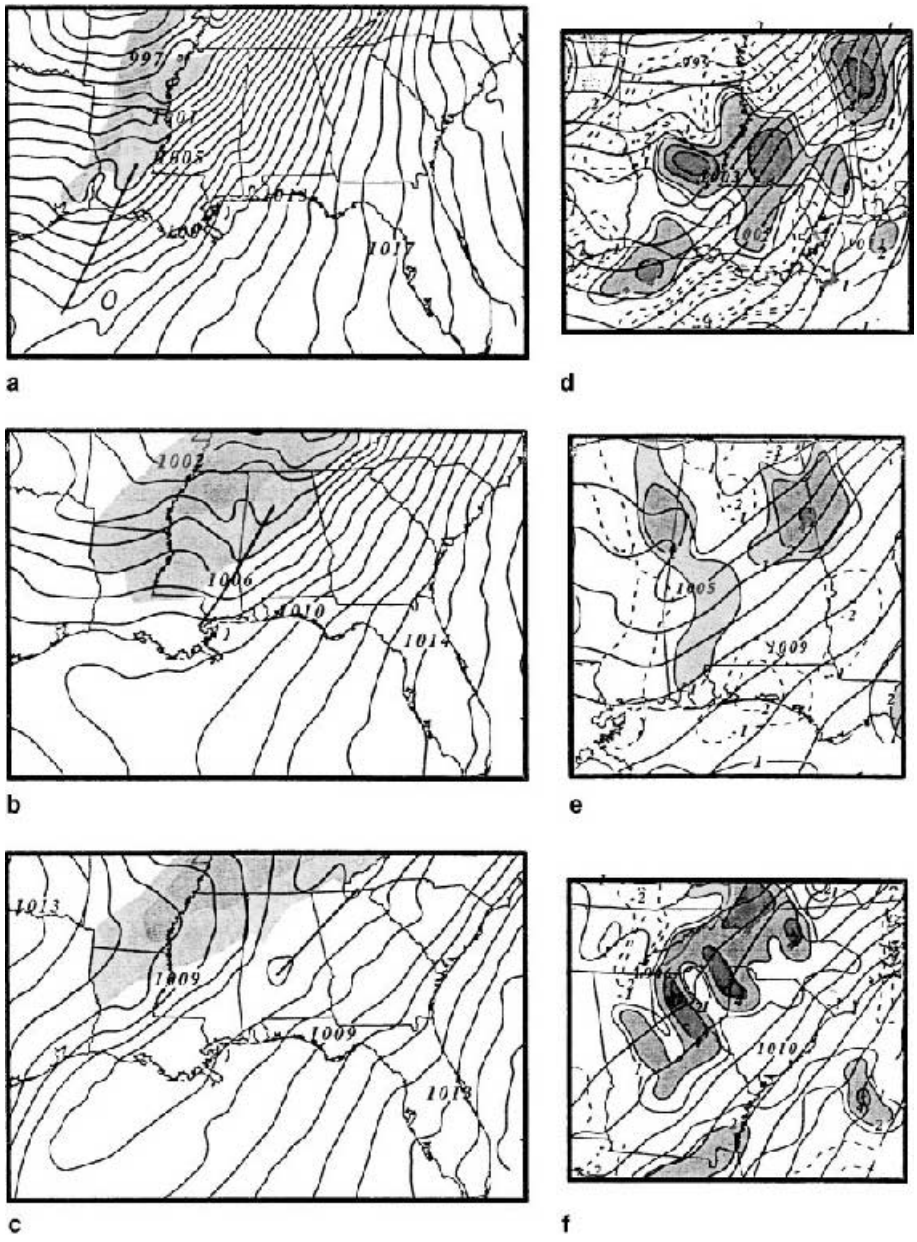

Fig. 19. MASS simulated, 24 km mesh, 600 hPa, wind isotachs (shaded at intervals of 5 for speeds greater than 35 ms^{-1}), mean sea-level pressure (solid lines, hPa) and analyzed trough (solid line) valid at **a** 1800 UTC 26, **b** 0600 UTC 27 and **c** 1800 UTC 27 November 1988. Mean sea-level pressure (thick solid lines, hPa) and 250 hPa divergence, contoured 1, 2, 4 & 6 (solid lines positive values and dashed lines negative values) and shaded greater than 1 ($\times 10^{-5}$ s^{-1}) valid at **d** 1800 UTC 26, **e** 0600 UTC 27, and **f** 1800 UTC 27 November 1988

the convection area and confluence zone, ascend rapidly, exit at a much higher level and they are greatly unbalanced with respect to the local environment. They accelerate in the mid-levels as evidenced by the wind barbs pointing toward the lower height field (subgeostrophy). This area of subgeostrophy creates mid-level divergence, which in turn helps maintain the low-level trough (confluence area). While the non-event case has a mid-level jet associated with the frontal boundary over AR and TN, it is much farther to the north than in the event case.

5. Potential vorticity

Potential vorticity may increase locally either by transport or generation. The generation of PV, through diabatic processes, may be examined using Eq. (1). In this section, we will discuss the generation, maintenance and propagation of the

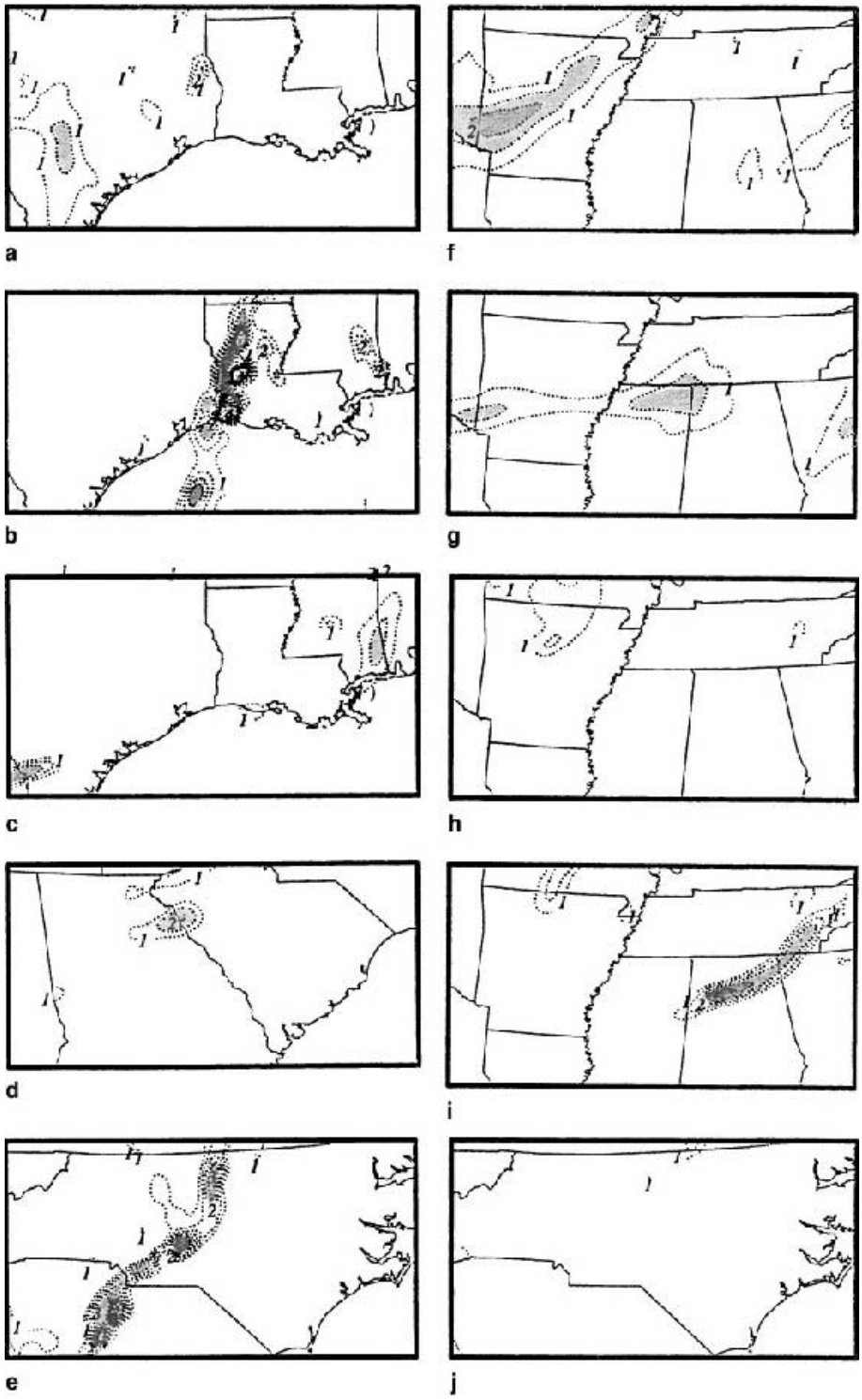

Fig. 20. Mass simulated, 24 km mesh 900 hPa PV (shaded greater than 1 PV unit by 0.5) valid at a. 0600 UTC 26, b. 1800 UTC 26, c. 0600 UTC 27, d. 1800 UTC 27, e. 0600 UTC 28 November 1988, f. 1800 UTC 23, g. 0600 UTC 24, h. 1800 UTC 24, i. 0600 UTC 25 and J. 0000 UTC 26 January 1990

low-level PV maximum for the event and non-event case. The low-level PV path is depicted in Fig 20.

5.1 Downward transport of potential vorticity

In the non-event case, there are several low-level PV maxima associated with the frontal boundary that extends across northern TX, AR and TN and within the PJ-entrance region. The PV is transported downward in the lee of the Rocky Mountains and associated with the PJ-entrance region (Fig. 21a). The upper-level PV maximum is located in the cold air, north of the left entrance region of the PJ. The distribution of PV

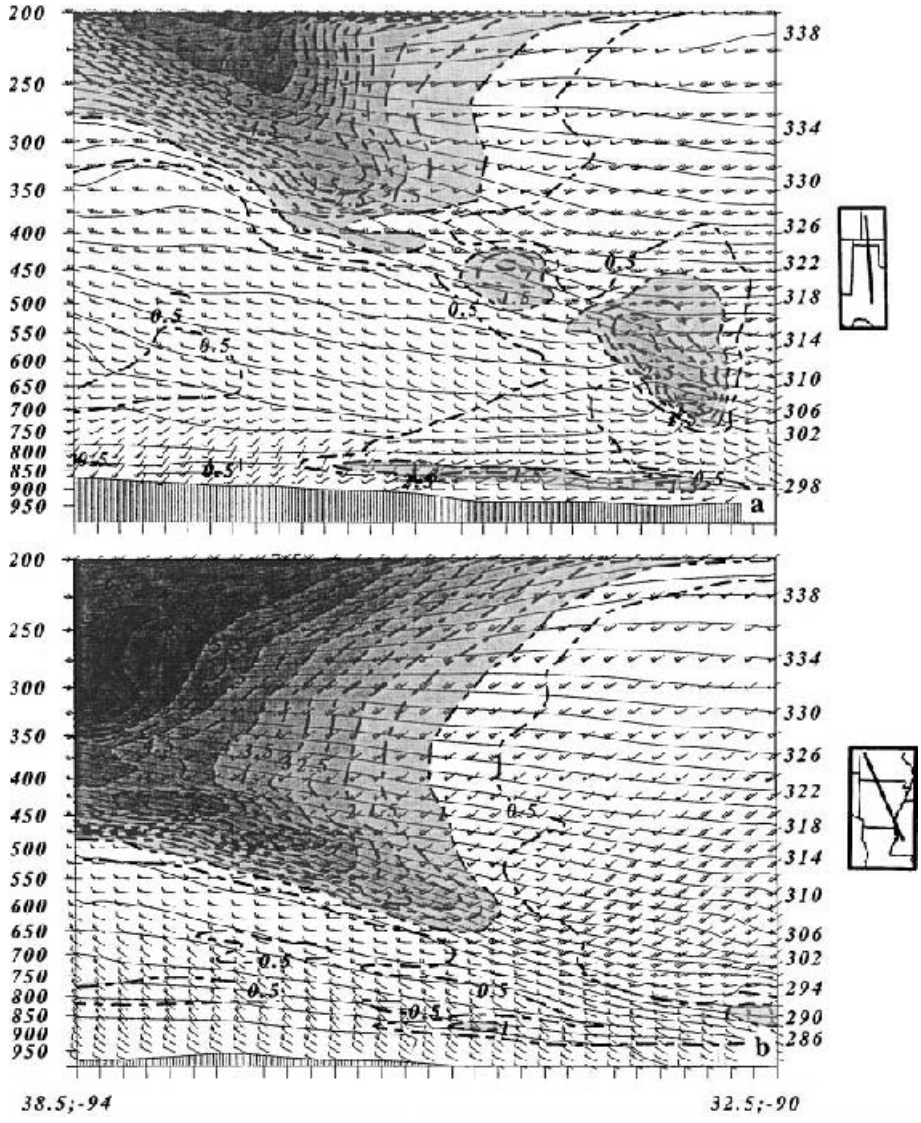

Fig. 21. MASS simulated, 24 km mesh, cross section including wind vectors (ms^{-1}), θ (solid lines, K), and PV (dashed lines, contoured greater than 0.5 and shaded greater than 1 PV units) **a** from 37N, 102.5W to 30.5N, 100W valid at 0300 UTC, and **b** from 38.5N, 94W to 32.5N, 90W valid at 0600 UTC 24 January 1990

resembles a tropopause fold (Danielsen, 1968). As the upper-level jet and surface front propagate eastward, there is a link between the upper-, mid- and low-level PV (Fig. 21b). A trajectory is constructed to show a parcel moving through the area of downward transport. Table 7 and Fig. 22 depicts the sinking motion of the air parcel. The PV distribution and parcel trajectory support the concept that the low-level PV originates and is maintained, in large part, by the downward transport of PV. The downward PV transport is not linked to any low-level forcing thus there is no rapid cyclogenesis.

In the event case, the PV maximum over the TX coast moves east over the Gulf Coast, then northeast to the Piedmont. The cross section valid 1500 UTC 26 November 1988 (Fig. 23) extends from eastern OK, bisects the strong low-level PV in eastern TX, and ends over the Gulf (south of LA). The upper- and mid-level PV maximum is associated with the intense thermal gradient located to the left of the PJ. The upper-level PV is not transported down to the low-levels. As the low-level PV maximum propagates along the Gulf Coast, the PV is maintained in the low-levels and builds vertically.

Figure 24a, b depicts the 900 hPa PV, sea level pressure and surface streamlines (confluence) for the event case at 1500 UTC 26 and 2100 UTC 27 Novembaer 1988, respectively. At 1500 UTC over TX and the western Gulf there exists an intense line of low-level PV associated with a surface

Table 7. Trajectory from 0100 UTC 24 January 1990 to 0500 UTC 24 January 1990. Trajectory was derived from hourly data of a 24 km MASS simulation. The following abbreviations are defined: Latitude (LAT), Longitude (LON), Pressure (PRS), Wind Speed & Direction (V_{total}), and Potential Vorticity (PV)

Time (UTC)	LAT (°N)	LON (°W)	PRS (hPa)	OMG 10^{-1}Pa s^{-1}	V_{total} (ms^{-1}) spd/dir	PV (PV units)
0100	36.8	97.8	364	0.252	41.4/273	0.5
0200	37	94.5	372	11.39	41.1/272	0.66
0300	36.8	94.5	397	10.98	40.4/269	1.45
0400	36.8	92.9	428	6.02	40.1/268	0.74
0500	36.9	91.3	439	0.265	39.7/265	0.42

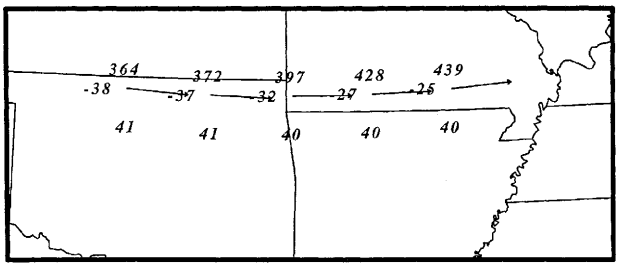

Fig. 22. Trajectory constructed from a 24 km MASS simulation. Station plots contain pressure (hPa), temperature (°C), and total wind speed (ms^{-1}). Displayed wind vectors depict total wind. Parcels initialized 0100 UTC and ended 0500 UTC 24 January 1990

trough (boundary between air masses) and convection. Figure 23 depicts a cross section perpendicular to the airmass boundary. The upper-level PV is separate from the low-levels and is not transported to the low-levels, which indicates the PV maxima are decoupled. By 2100 UTC 27 November 1988 the NWS analysis modifies the trough to a cold front over the Gulf States. A frontal boundary can be analyzed in the simulated data. The strongest PV is over the southern portion of the cold front (where the confluence zone was last analyzed) while the northern portion of frontal system does not have any associated low-level PV. The low-level PV maximum propagating along the Gulf Coast maintains its integrity.

In summary, the low-level PV maximum is maintained in the low-levels in the event case. In the non-event case, the low-level PV originates and is maintained, in part, by continuous downward transport of PV associated with the PJ entrance region.

5.2 Possible energy sources maintaining the low-level potential vorticity

We examine other potential energy sources (diabatic heating, thermal and wind shear gradients) and their relationship to the low-level PV. These energy sources act to produce and/or maintain the PV via term 3 in Eq. (1). Low-level PV maxima (>1 PV unit) are associated with strong vertical and horizontal wind shear gradients, localized areas of strong potential temperature gradients, and confluence areas. In this section we switch to a Lagrangian frame of reference. The relative contribution of each term in the PV Eq. (1) is evaluated in a manner analogous to Kaplan and Karyampudi (1992b) using parcel trajectory data with the exception of the gradient field which is calculated using a centered finite differencing scheme about the center trajectory point. Using trajectories, we examine the PV maximum at the beginning of this time period (over southeast LA at 0000 UTC 26 November 1988) and late in this time period (over central AL at 1000 UTC 27 November 1988).

The parcel over southeastern LA originates in the PV maximum and moves northeastward (Table 8) encountering higher environmental PV. Convection is present over LA for the first 3 hours of the trajectory generating a large amount of latent heating. The relative contribution of each term in the PV Eq. (1) is evaluated. Term one contributes 37% to the production of PV by the change in static stability associated with the latent heating or the surface sensible heating in a well-mixed layer. Term two contributes 22% to the change in PV resulting from horizontal gradients of diabatic heating within regions of wind covariances (friction).

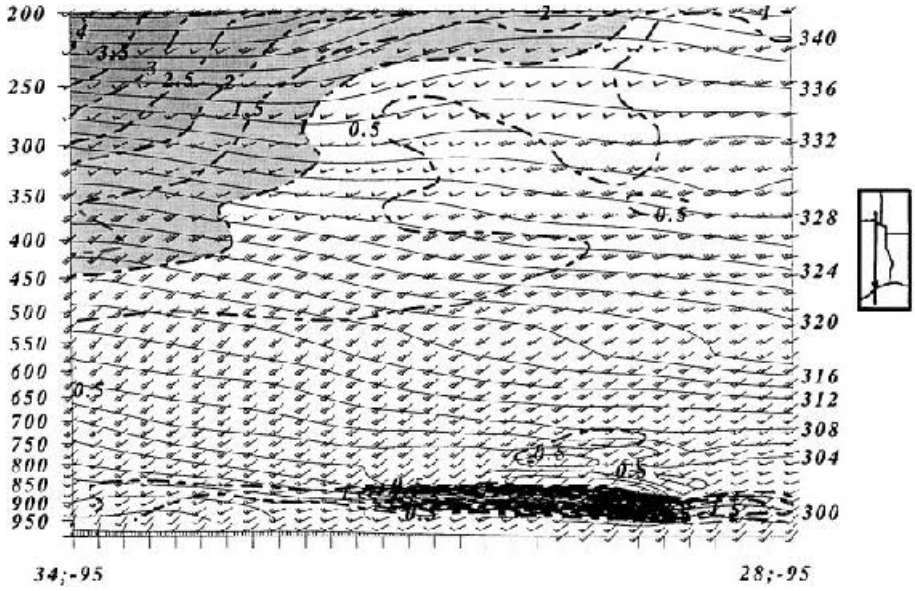

Fig. 23. MASS simulated, 24 km mesh, cross section including wind vectors (ms^{-1}), θ (solid lines, K), and PV (dashed lines, contoured greater than 0.5 and shaded greater than 1 PV units) from 34N, 95W to 28N, 95W valid at 1500 UTC 26 November 1988

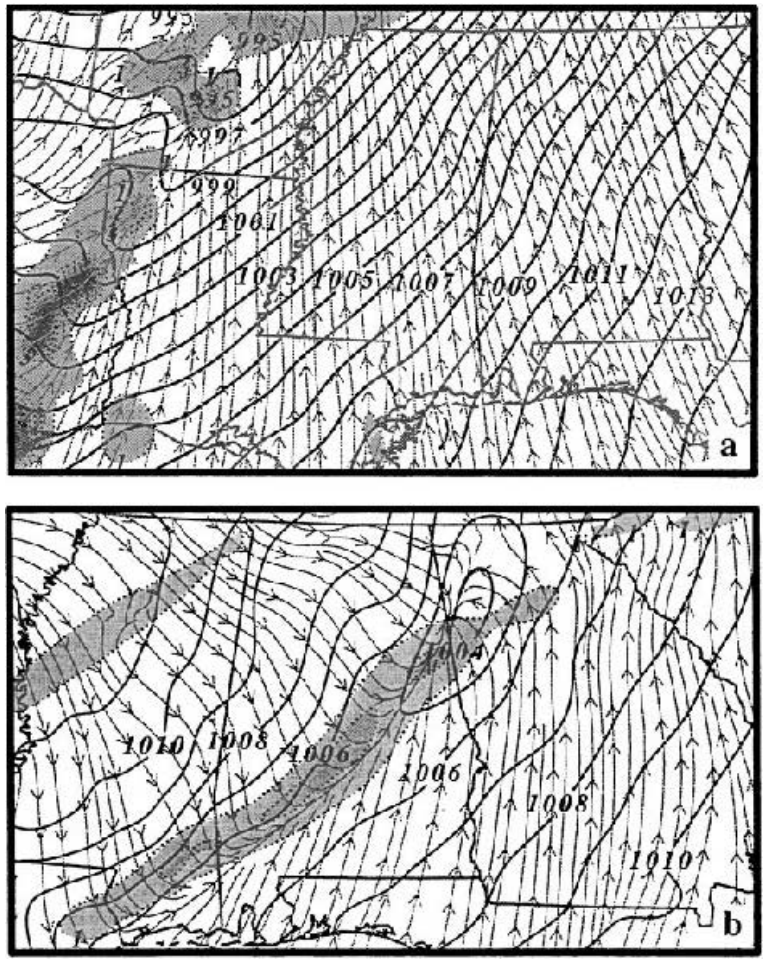

Fig. 24. MASS simulated, 24 km mesh, 900 hPa PV (shaded greater than 1 by 0.5 PV units), sea-level pressure (solid lines, hPa) and surface streamlines valid at **a** 1500 UTC 26, and **b** 2100 UTC 27 November 1988

Table 8. Trajectory from 2200 UTC 26 November 1988 to 0300 UTC 27 November 1988 Trajectory was derived from hourly data of a 24 km MASS simulation. The following abbreviations are defined: Latitude (LAT), Longitude (LON), Pressure (PRS), Temperature (TMP), and Potential Vorticity (PV)

Time (UTC)	LAT (°N)	LON (°W)	PRS (hPa)	TMP (°C)	PV (PV units)
26/2200	29.66	92.36	894.3	17.79	1.548
26/2300	29.37	91.71	895.2	17.42	1.470
27/0000	30.25	91.25	899.4	17.24	2.138
27/0100	30.58	90.72	905.4	17.41	2.074
27/0200	30.94	90.20	907.3	17.06	2.282
27/0300	31.35	89.69	905.5	16.42	2.353

Table 9. Trajectory from 0600 UTC 27 November 1988 to 1000 UTC 27 November 1988. Trajectory was derived from hourly data of a 24 km MASS simulation. The following abbreviations are defined: Latitude (LAT), Longitude (LON), Pressure (PRS), Temperature (TMP), and Potential Vorticity (PV)

Time (UTC)	LAT (°N)	LON (°W)	PRS (hPa)	TMP (°C)	PV (PV units)
27/0600	31.29	88.01	944.9	19.16	0.06716
27/0700	31.79	87.62	939.9	18.78	0.1112
27/0800	32.29	87.20	939.7	18.78	0.2298
27/0900	32.76	86.75	902.8	15.22	13.33
27/1000	33.17	86.25	846.2	12.37	3.329

Term three contributes 41% to the production of PV resulting from the tilting of the horizontal component of vorticity into the vertical through horizontal diabatic heating. In this case, the parcel experiences growing stretching and tilting as it ascends in conjunction with the surface trough and convection, which generates PV.

We follow the PV maximum as it moves over central AL and send a parcel through the PV maximum at 0900 UTC. The parcel's PV increases from 0.2298 PV units to 13.33 PV units from 0800 to 0900 UTC (Table 9). Figure 25 depicts the parcel trajectory, PV maximum and latent heating associated with convection. By 0800 UTC 27 November 1988 the surface trough (confluence zone) is over central AL. The greatest PV increase occurs when the parcel moves through a latent heating maximum (>10 °Ch^{-1}) at 0900 UTC. Sensible heating is negligible at this time. Latent heating increases the low-level PV.

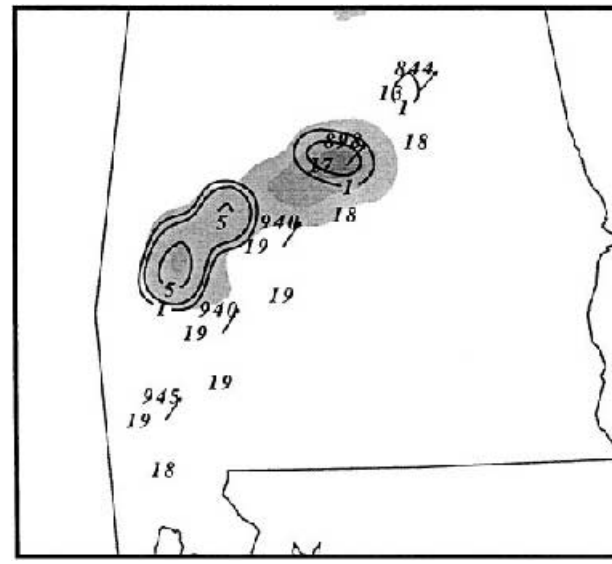

Fig. 25. Trajectory constructed from a 24 km MASS simulation initialized at 0600 UTC and ending at 1000 UTC 27 November 1988 plotted over convective latent heating (contoured at 1, 2, 5, 10, 15, 20 C h^{-1}) at 900 hPa. Station plots contain pressure (hPa), temperature (C), and total wind speed (ms^{-1}). Displayed wind vectors depict total wind

The non-event case has several PV maxima moving out of western OK, across TN and into VA. These maxima weaken as they propagate across the central part of the country. A final PV maximum develops over central MS and propagates over northern AL and into TN (Fig. 20h). This low-level PV maximum develops rapidly over 6 hours as it moves into central AL and is associated with convection. A MASS simulation without latent heating is completed to investigate this PV maximum. Figure 26 depicts the 900 hPa PV distribution (without latent heating) over the southeast US. The PV maximum over AR and MO is not altered in the simulation without latent heating supporting the concept that this PV maximum is maintained by downward transport of stratospheric PV. However, the PV maximum (with latent heating) over LA and MS does not exist indicating that this PV maximum is dependent on convection.

In summary, in the non-event case there are numerous PV maxima originating in the lee of the Rocky Mountains and move eastward into VA. The upper-level PV maximum is located in the cold air, north of the left entrance region of the PJ and the PV distribution resembles a

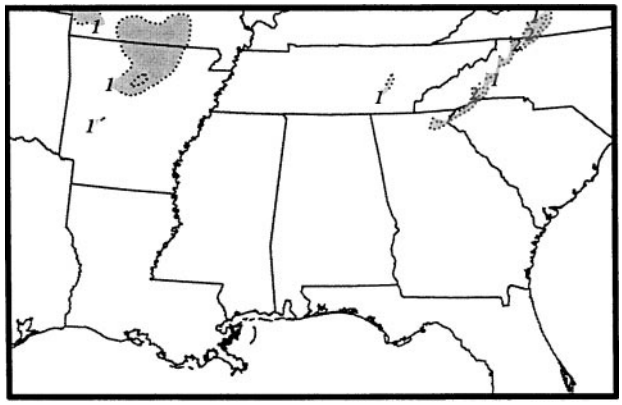

Fig. 26. MASS simulated, without latent heating, 24 km mesh, 900 hPa level PV (shaded greater than 1 by 0.5 PV units) valid at 1800 UTC 24 January 1990

tropopause fold. The PV distribution and upper-level sinking support the concept that the low-level PV originates and is maintained, in large part, by the downward transport of stratosphere PV. A final PV maximum associated with convection develops over central MS and moves northeastward to TN. In the event case, the PV maximum over the TX coast (originates from central MX) moves eastward across the Gulf, then northeastward to the Piedmont. The PV is maintained in the low-levels, builds vertically and is associated a surface trough (confluence) and convection. As the low-level PV maximum propagates along the Gulf Coast it is maintained by low-level mechanisms. The upper-level PV is not transported down to the low-levels.

6. Concluding remarks

Observed data and model simulations highlight the differences between the event and non-event cases and the relationship between the upper-level jets and convection. In the event case, a STJ was located over the Gulf Coast region. The upper-level wind was subgeostrophic over the north TX coast, LA and MS indicating acceleration and divergence, which facilitated ascent and deep convection. In the non-event case, there was a strong PJ over northern TX extending northeast. The upper-level wind was supergeostrophic over the TX coast, LA, MS and AL indicating deceleration, convergence and sinking, which inhibited deep convection.

The mid-level jet also differed between these cases. In the event case, a mid-level jet developed over TX and moved eastward across the southern states, from TX to GA. The jet developed rapidly over eastern TX in response to the increased PGF, which developed as the trough propagated eastward over the Midwestern states while the warm Mexican airmass maintained the heights over the Gulf Coast. The environment was predisposed to produce a midlevel jet due to the warm, low-level airmass that moved from the Mexican plateau to the Gulf Coast near the TX/LA border. The mid-level jet right entrance region was closely associated with the surface trough. The thermally direct ageostrophic circulation enhanced ascent over the surface trough, which helped maintain the trough and convection.

In the non-event case, there were two distinct mid-level jets covering two time periods. First, until approximately 0600 UTC 25 January 1990, there was a narrow mid-level jet that extended across northern LA, MS, AL and TN. The jet was closely associated with the surface front and a narrow band of cold air advection and a strong height gradient. After 0600 UTC 25 January 1990 a second mid-level jet developed over the Tennessee Valley Region, which was associated with a balanced, QG system.

Observed data and model simulations highlight the surface differences between the event and non-event cases. The event case had strong surface confluence, a meso-trough and strong convection that propagated across the Gulf Coast states. The upper-level divergence and the thermally direct circulation about the mid-level jet created ascent, which helped to maintain the surface trough and convection. In the non-event case, there was a quasi-stationary front and mid-level jet over OK, AR, TN and KY. Also, there was a weak surface frontal system (trough) over the Gulf Coast. There was upper-level convergence over the Gulf Coast, which inhibited the deep convection.

There are differences between the origins and maintenance of the low-level PV between these two cases. In the non-event case, several PV maxima originated in the lee of the Rocky Mountains and moved eastward to VA. The PV distribution and the upper-level sinking support the concept that the low-level PV originated and

is maintained, in large part, by the downward transport of stratospheric PV (tropopause fold). However, the downward transport of PV is not linked to any strong low-level forcing thus there is not any rapid cyclogenesis. Late in the period, another PV maximum developed in association with convection over central MS and it moved northeast to the Appalachians. In the event case, the low-level PV maximum over the TX coast propagated eastward across the Gulf then northeast to the Piedmont. The low-level PV maximum was associated with a surface trough, confluence, convection and was primarily maintained by tilting effects associated with diabatic heating.

In summary, the mid-period of the event case had a self-maintaining, low-level circulation that originated over Mexico, propagated across the Gulf Coast and moved over the Piedmont at the time of the tornado outbreak. This circulation moved across the Gulf Coast States as a coherent feature and was characterized by a surface trough, low-level PV maximum, mid-level jet, a warm Mexican airmass and upper-level divergence associated with the STJ, In the non-event case, these features were absent along the Gulf Coast states.

Acknowledgements

The first author would like to thank the Air Force Institute of Technology for the opportunity to pursue my advanced degree. The authors wish to thank Drs Robert Rozumalski and Kenneth Waight III of MESO Inc. for access to and help with the MASS model.

References

Daley R (1991) Atmospheric Data Analysis. Cambridge: Cambridge University Press, 457 pp

Danielsen E (1968) Stratospheric-tropospheric exchange based on radioactivity, ozone, and potential vorticity. J Atmos Sci 25: 502–518

Egentowich JM, Kaplan ML, Lin Y-L, Riordan AJ (1999a) Mesoscale simulations of dynamical factors discriminating between a tornado outbreak and non-event over the southeast US, part I: 84 – 48 hour precursors. Meteorol Atmos Phys (current issue)

Fawbush EJ, Miller RC (1954) The types of airmasses in which North American tornadoes form. Bull Amer Meteor Soc 35: 154–165

Gidel LT, Shapiro MA (1979) The role of clear air turbulence in the production of potential vorticity in the vicinity of upper tropospheric jet stream-frontal systems. J Atmos Sci 36: 2125–2138

Gonski RF, Woods BP, Korotky WD, (1989) The Raleigh tornado – 28 November (1988) An operational perspective. Preprints, 12th Conf. on Weather Analysis and Forecasting, Monterey, CA Amer Meteor Soc, pp 173–178.

Gyakum JR, Kuo Y-H, Gao Z, Guo YR (1995) A case of rapid continental mesoscale cyclogenesis. Part II: Model and observational diagnosis. Mon Wea Rev 123: 998–1024

Kalnay E, Kanamistu M, Kistler R, Collins W, Deaven D, Gandin L, Iredell M, Saha S, White G, Woolen J, Zhu Y, Chelliah M, Ebisuzaki W, Higgins W, Janowiak J, Mo K C, Ropelewski C, Wang J, Leetmaa A, Reynolds R, Jenne R, Joseph D (1996) The NMC/NCAR 40-year reanalysis project. Bull Amer Meteor Soc 77(3): 437–471

Kaplan ML, Paine DA (1977) The observed divergence of the horizontal velocity field and pressure gradient force at the mesoscale. It's implications for the parameterization of three-dimensional momentum transport in synoptic-scale numerical models. Beitr Phy Atmos 50: 321–330

Kaplan ML, Karyampudi VM (1992a) Meso-beta numerical simulation of terrain drag-induced along stream circulations. Part I: Midtropospheric frontogenesis. Meteorol Atmos Phys 49: 133–156

Kaplan ML, Karyampudi VM (1992b) Meso-beta numerical simulation of terrain drag-induced along stream circulations. Part II: Concentration of potential vorticity within dryline bulges. Meteorol Atmos Phys 49: 157–185

Kaplan ML, Zack JW, Wong VC, Tuccillo JJ (1982a) Initial results from a mesoscale atmospheric simulation system and comparisons with the AVE-SESAME I data set. Mon Wea Rev, 110: 1564–1590

Kaplan ML, Lin Y-L, Hamilton DW, Rozumalski RA (1998) The numerical simulation of an unbalanced jetlet and its role in the Palm Sunday (1994) tornado outbreak in Alabama and Georgia. Mon Wea Rev 126: 2133–2165

Keyser D, Shapiro MA (1986) A review of the structure and dynamics of upper-level frontal zones. Mon Wea Rev 114: 452–499

Lanicci JM, Warner TT (1991a) A synoptic climatology of the elevated mixed-layer inversion over the southern Great Plains in Spring. Part 1: Structure, dynamics, and seasonal evolution. Wea & Forecasting 6: 181–197

Lanicci JM, Warner TT (1991b) A synoptic climatology of the elevated mixed-layer inversion over the southern Great Plains in Spring. Part 2: the life cycle of the lid. Wea & Forecasting 6: 198–213

Lanicci JM, Warner TT (1991c) A synoptic climatology of the elevated mixed-layer inversion over the southern Great Plains in Spring. Part 3: Relationship to severe-storms climatology. Wea & Forecasting 6: 214–226

Lin Y-L, Farley RD, Orville HD (1983) Bulk parameterization of the snow field in a cloud model, J Clim Appl Meteorol 22: 1065–1092

Mahrt L, Pan H (1984) A two-layer model of soil hydrology. Bound-Layer Meteor 29: 1–20

MESO (1995) MASS Version 5.8 Reference Manual, MESO, Troy, NY, 199 pp

NOAA (1988) Storm data 30(11): 72 pp

Noilhan J, Planton S (1989) A simple parameterization of and surface processes for meteorological models. Mon Wea Rev 117: 536–549

Rozumalski RA (1997) The role of jet streak regeneration forced by a deepening continental planetary boundary layer in the explosive surface cyclogenesis of 28 March 1984. PhD Thesis, North Carolina State University, 360 pp (Available from the corresponding author)

Uccellini LW, Johnson D (1979) The coupling of upper and lower tropospheric jet streaks and implication for the development of severe convective storms. Mon Wea Rev 107: 682–703

Uccellini LW, Kocin PJ (1987) The interaction of jet streak circulations during heavy snow events along the East Coast of the United States. Wea & Forecasting 1: 289–308

Uccellini LW, Kocin PJ, Petersen RA, Wash CH, Brill KF (1984) The President's day cyclone of 18–19 February 1979: Synoptic overview and analysis of the subtropical jet streak influencing the pre-cyclogenetic period. Mon Wea Rev 112: 31–55

Zang DL, Anthes RA (1982) A high resolution model of the planetary boundary layer-sensitivity tests and comparisons with SESAME-79 data. J Appl Meteor 21: 1594–1609

Zehnder JA, Keyser D (1991) The influence or interior gradients of potential vorticity on rapid cyclogenesis. Tellus 43A: 198–212

Corresponding author's address: Dr. Yuh-Lang Lin, Department of Marine, Earth and Atmospheric Sciences, North Carolina State University, Raleigh, NC 27695-8208 (E-Mail: yl_lin @ncsu.edu)